Journal of Environmental Chemical Engineering 10 (2022) 107442

Contents lists available at ScienceDirect

Journal of Environmental Chemical Engineering

journal homepage: www.elsevier.com/locate/jece

Multistage treatment for olive mill wastewater: Assessing legal compliance and operational costs

Srikanth Vuppala [a,1], Larissa O. Paulista [b,c,1], Daniela F.S. Morais [b,c,*], Inês L. Pinho [b,c], Ramiro J.E. Martins [b,c,d], Ana I. Gomes [b,c,*], Francisca C. Moreira [b,c], Vítor J.P. Vilar [b,c,*]

[a] Department of Civil and Environmental Engineering, Politecnico di Milano, Piazza Leonardo da Vinci, 32, 20133 Milan, Italy
[b] Laboratory of Separation and Reaction Engineering - Laboratory of Catalysis and Materials (LSRE-LCM), Faculty of Engineering, University of Porto, Rua Dr. Roberto Frias, 4200-465 Porto, Portugal
[c] Associate Laboratory in Chemical Engineering (ALiCE), Faculty of Engineering, University of Porto, Rua Dr. Roberto Frias, 4200-465 Porto, Portugal
[d] Departamento de Tecnologia Química e Biológica, Escola Superior de Tecnologia e Gestão, Instituto Politécnico de Bragança, Campus de Santa Apolónia, 5300-253 Bragança Portugal

ARTICLE INFO

Editor: Despo Kassinos

Keywords:
Advanced oxidation processes
Biological oxidation
Coagulation
Integrated treatment
Real wastewater
Operational costs

ABSTRACT

A treatment train for the remediation of a raw olive mill wastewater (OMW) was investigated, aiming to comply with the emission limit values (ELVs) for direct discharge into water bodies. The following stages were proposed: (i) pre-treatment (filtration and sedimentation), (ii) coagulation, (iii) biological oxidation, and (iv) advanced oxidation process (AOP). Under the best-operating conditions for coagulation (0.8 g L^{-1} of $Al_2(SO_4)_3$, pH = 4.5), high removal of total suspended solids (TSS) (97%), turbidity (98%), and phenols (57%) was achieved, along with a decrease in the inhibition of the biological activity. A subsequent biological oxidation stage provided a high removal of organic matter (chemical oxygen demand (COD) removal of 73%). For the third stage, three AOPs were applied and compared – photo-Fenton with UVA radiation (PF-UVA), anodic oxidation (AO), and ozonation (O_3). After 3 h of treatment, the PF-UVA process (pH = 2.8, $[H_2O_2]$ = 400–500 mg L^{-1}, [Total dissolved iron]$_0$ = 100 mg L^{-1}) allowed to meet the ELV for COD, but the other parameters exceeded the threshold, while O_3 process (inlet concentration = 100 mg O_3 Ndm^{-3}, gas flow = 0.2 Ndm^3 min^{-1}) allowed to comply with phenols, TSS, and sulfate limits. The AO process (current density up to 200 mA cm^{-2}) was the least efficient AOP for all studied parameters. The operational costs for the coagulation and biological oxidation stages were estimated at 1.20 € m^{-3}. Regarding the most effective AOPs, ozonation presented an estimated cost 2.3-fold higher than PF-UVA (11.9 € m^{-3} *vs.* 5.2 € m^{-3}).

1. Introduction

The olive oil industry is highly relevant for the European Union economy, contributing to around two-thirds of the World's production over the last decade. Portugal is the fourth biggest producer of olive oil in Europe, providing about 4% and 3%, respectively, of the European and World production [1]. Even though the olive oil industry is one of the most important sectors in the agro-food industries, benefiting socio-economically the producing countries, it generates one of the most polluting wastewaters: the olive mill wastewater (OMW) [2,3]. According to the International Olive Council (IOC), 2019/20 crop year production was 3.2 × 10^9 m^3 OMW, with the same estimation for 2020/21 [4].

Olive oil is extracted from the fresh fruit of the olive tree by traditional pressing or two/three-phase centrifugal processes. OMW composition and quantity vary with the technology used, being the two-phase system the most eco-friendly one since it dramatically reduces the volume of effluent generated [5,6]. However, OMW is highly toxic to the environment because of its (i) high acidity (pH range between 3 and 6), and (ii) high organic load (4–18% w/w). This organic fraction comprises some growth-inhibitor compounds that are difficult to biodegrade, such as phenolic compounds (total phenolic compounds, TPh, 2–15% w/w),

* Corresponding authors at: Associate Laboratory in Chemical Engineering (LSRE-LCM and ALiCE), Faculty of Engineering, University of Porto, Rua Dr. Roberto Frias, 4200-465 Porto, Portugal.
E-mail addresses: daniela.morais@fe.up.pt (D.F.S. Morais), ana.isabelgomes@fe.up.pt (A.I. Gomes), vilar@fe.up.pt (V.J.P. Vilar).
[1] The first two authors contributed equally to this work.

https://doi.org/10.1016/j.jece.2022.107442
Received 6 December 2021; Received in revised form 17 February 2022; Accepted 18 February 2022
Available online 23 February 2022

Table 1
Survey of research on multistage treatments applied to OMWs.

Multistage treatment strategy	Operational conditions	Efficiency	Reference
Acid cracking + Coagulation + O_3/UV	Acid cracking: $[H_2SO_4] = 5$ mL L^{-1} Coagulation: pH = 8; $[FeCl_3.6\ H_2O] = 3$ g L^{-1} O_3/UV: pH = pH = 7; $[O_3] = 0.3$ g h^{-1}; $t = 440$ min	COD removal = 98% Phenols removal = 99%	[13]
Acid cracking + Coagulation + UV/H_2O_2	Acid cracking: $[H_2SO_4] = 5$ mL L^{-1} Coagulation: pH = 8; $[FeCl_3.6\ H_2O] = 3$ g L^{-1} UV/H_2O_2: pH = 2; $[H_2O_2] = 0.75$ g L^{-1}; $t = 720$ min	COD removal = 99% Phenols removal = 99%	
Acid cracking + Coagulation + Fenton	Acid cracking: H_2SO_4; pH = 2.5 Coagulation: pH = 9; $[FeCl_3] = 6$ g L^{-1} Fenton: pH = 3; $[Fe^{2+}] \approx 1$ g L^{-1}; $[H_2O_2] \approx 12$ g L^{-1}; $t = 240$ min	COD removal = 83% Phenols removal = 98.6%	[19]
Coagulation/flocculation + Fenton	Coagulation: pH = 5; [P19][a] = 1 g L^{-1}; [2045-SH][b] = 0.1 g L^{-1} Fenton: $[FeSO_4.7\ H_2O] = 3.5$ g L^{-1}; $[H_2O_2] = 7.14$ g L^{-1}	COD removal = 90% Phenols removal = 92%	[11]
Coagulation + Fenton	Coagulation: pH = 9; [PDADMAC][c] = 40 mg L^{-1} Fenton: $[Fe2^{+}] = 2$ g L^{-1}; $[H_2O_2] = 4$ g L^{-1}; $t = 60$ min	COD removal = 45%	[20]
Coagulation + PF	Coagulation: pH = natural (4.3); [Chitosan] = 0.4 g L^{-1} PF: pH = 3; H_2O_2:$FeSO_4$ = 8.1 (w/w) (15,000:1852); $t = 30$ min	COD removal = 93%	[21]
Coagulation/flocculation + Dilution + Solar PF	Coagulation/flocculation: pH ≈ 5; $[FeSO_4.7\ H_2O] = 6.67$ g L^{-1}; [FLOCAN 23] = 0.287 g L^{-1} Dilution: 30-fold Solar PF: pH = 2.8–2.9; $[Fe^{2+}] = 0.08$ g L^{-1}; $[H_2O_2] = 1.0$ g L^{-1}; $t = 240$ min	COD removal = 94% Phenols removal = 99.8%	[22]
Sedimentation + Fenton + Coagulation/flocculation	Sedimentation: 12 h Fenton: pH = 3.0; Fe^{3+}:$H_2O_2 = 0.04$ ($[Fe^{3+}] = 1.0$ g L^{-1}; $[H_2O_2] = 25$ g L^{-1}); $t = 180$ min Coagulation: $FeCl_3$ used as both catalyst and coagulant	COD removal = 77% Phenols removal = 96%	[5]
Dilution + Sedimentation + Fenton + Anaerobic biological treatment	Dilution: 2-fold Sedimentation: 1–2 h Fenton: pH = 2; Fe^{2+}:H_2O_2 molar ratio = 1:50 Anaerobic biological treatment: 2 stage upflow treatment; sludge residence time = 100 d (1st stage) + 133.3 d (2nd stage); hydraulic retention time = 24 h each; $T = 16$–30 °C;	COD removal = 77% Phenols removal = 57%	[23]
Dilution + O_3 + aerobic process w/ encapsulated biomass	Dilution: 10-fold O_3: pH = 4.85; $OD_T = 765$ mg O_3 L^{-1}; $t = 60$ min Aerobic process: 0.8 × 2.5 cm capsules of celulose acetate microfiltration membrane; $t = 48$ h	COD removal = 36% Phenol removal = 61%	[24]

[a]P19 – cationic organic coagulant; [b]2045-SH – anionic flocculant; [c]PDADMAC - polydiallyldimethylammonium chloride.

sugars, organic acids, proteins, and lipids. The most recalcitrant portion of the OMW is the polymeric phenol, also responsible for the dark-brown color of the effluent [3, 5–11]. Environmental problems of OMW disposal are related to ground and surface water pollution, odor nuisance, among others. These problems are increasing as a result of a lack of common international laws, but also as a result of the seasonal and geographical nature of the production [3,5,6,10]. As a result, suitable treatment strategies are needed for OMW remediation.

Different treatment processes have been investigated over the years, from (i) biological processes (aerobic and/or anaerobic operation) [7], to (ii) physicochemical methods (coagulation, coagulation/flocculation, acid cracking) [12], and (iii) advanced oxidation processes (AOPs), like photocatalysis [8], ultraviolet radiation coupled to hydrogen peroxide oxidant (UV/H_2O_2) [13], Fenton/photo-Fenton (PF) reactions [9,14, 15], ozonation (O_3) [13,16,17], and electrochemical methods, such as anodic oxidation (AO) [18] and electro-Fenton (EF) [10]. Although OMW treatment has been the focus of many research studies, only a few of them attempt to combine different treatment processes (Table 1). Of these, most use coagulation followed by an AOP (usually single Fenton or PF), and few apply a biological treatment, commonly on the last treatment stage. Also, as a result of the high organic load and high biological inhibition of OMW, most of the studies reported in the literature use a diluted effluent.

The present work aims to develop a treatment train for the remediation of a raw-undiluted OMW, with underlying concerns regarding compliance with the emission limit values (ELVs) for direct discharge into environmental compartments and the economic feasibility of the proposed treatment processes (key aspects for decision-makers when dealing with these effluents). Coagulation/flocculation processes, biological oxidation, and three AOPs – PF with UVA radiation (PF-UVA), AO and O_3 – were tested under different operational conditions.

2. Material and methods

2.1. Chemicals

Aluminum sulfate ($Al_2(SO_4)_3$) 48% (w/w) from Rivaz Química and ferric chloride ($FeCl_3$) 40% (w/v) from Quimitécnica were used as coagulants. Chitosan solution was also used as coagulant, being prepared by dissolving chitosan 99.9% (w/w) from Sigma Aldrich in a mixture of 2 M hydrochloric acid (HCl) 37% (w/w) and deionized water, following the procedure in Vuppala, *et al.* [25]. Cationic Ambifloc 5351 UUJ and Superfloc C-492, and anionic polyacrylamide Magnafloc 155 (all from Tratamento de Águas, Lda.) were used as flocculant agents. PF experiments were performed using iron(II) sulfate heptahydrate ($FeSO_4.7\ H_2O$) 98% (w/w) from Panreac as iron source and H_2O_2 30% (w/v) from Fisher Chemical as oxidant. Sodium sulfite (Na_2SO_3) from Merk was used to quench the remaining H_2O_2 from the sample solution before analysis. Sodium chloride (NaCl) > 97% (w/w) supplied by Merck was used in an AO trial to increase the supporting electrolyte conductivity. Potassium iodide (KI) 100% (w/w) from VWR was used to vent the residual O_3 gas in ozonation trials. Sulfuric acid (H_2SO_4) 98% (w/w) and sodium hydroxide (NaOH) ≥ 99% (w/w) from Sigma-Aldrich were applied for pH adjustments. Standards for ion chromatography were purchased from Sigma-Aldrich and Fluka. Potassium hydroxide (KOH) 1 M from Thermo Fisher Scientific and methanesulfonic acid (CH_4O_3S) ≥ 99% (w/w) from Merck were applied as eluents in ion chromatography. All chemicals were of analytical grade. Ultrapure and demineralized water used in analytical determinations were obtained from a Millipore® Direct-Q system (18.2 MΩ cm resistivity at 25 °C) and a reverse osmosis system (Panice), respectively.

2.2. Olive mill wastewater

The raw OMW (r-OMW) was collected from an olive oil production plant in Northern Portugal, which adopted a two-phase centrifugation process for oil extraction. The r-OMW was collected 1 m deep from the storage tank and filtered through a 2 mm pore sieve to remove the largest solids in suspension. Then, it was settled for ca. one week, allowing the separation of (from top to bottom) (i) oil and grease, (ii) OMW effluent, and (iii) sludge and solids. Accordingly, oil and grease were top removed, and the effluent supernatant was carefully withdrawn, obtaining a pre-treated OMW (p-OMW), which was used in the subsequent treatments. The main physicochemical characteristics of p-OMW used in this work are presented in Table 2. Note that the proper characterization of the r-OMW was unfeasible due to the large amount of

Table 2
Main physicochemical characteristics of the OMW after each treatment stage.

Parameter	Units	p-OMW[a]	c-OMW[b]	bio-OMW[c]	AOPs			ELV[g]
					PF-UVA[d]	AO[e]	O_3[f]	
pH	Sorënsen scale	4.5	4.5	8.3	2.8	9.3	8.3	6.0–9.0
Color	mg Pt-Co L^{-1}	n.m.	n.m.	1340	110	420	< 12 [h]	–
Color (1:20 dilution)	–	d.	d.	d.	n.d.	n.d.	n.d.	n.d.
Chemical oxygen demand – COD	mg O_2 L^{-1}	10,070	8071	718	68	440	167	150
Dissolved organic carbon – DOC	mg C L^{-1}	2940	2430	319	50	223	113	–
COD/DOC	–	3.4	3.3	2.3	1.4	2.0	1.5	–
Biodegradability (28-day of Zhan-Wellens test) (1:2 / 1:10 dilution)	%	49 / 77	91 / 88	n.m.	n.m.	n.m.	n.m.	n.m.
Aromatic compounds – UV_{254} (1:20)	A.U.	n.m.	n.m.	0.331	0.072	0.158	0.012	–
$SUVA_{254}$	L mg^{-1} m^{-1}	n.m.	–	2.1	2.9	1.5	0.2	–
Total suspended solids – TSS	mg L^{-1}	3990	120	105	260	99	47	60
Volatile suspended solids – VSS	mg L^{-1}	550	23	43	135	48	7	–
Turbidity	NTU	4600	80	120	150	170	15	–
Phenols	mg C_6H_6O L^{-1}	164	70	5.3	2.2	1.6	0.5	0.5
Chloride – Cl^-	mg L^{-1}	457	464	589	548	n.m.	572	–
Sulfate – SO_4^{2-}	mg L^{-1}	82	518	1933	3144	1800	1883	2000
Sodium – Na^+	mg L^{-1}	867	313	1373	1333	n.m.	1412	–

[a] OMW after pre-treatment (p-OMW) (it was unfeasible to properly characterize the raw OMW due to the large amount of sludge and solids, and oil and grease). Conditions: filtration through a 2 mm pore sieve followed by ca. two days settling; [b] OMW after coagulation process (c-OMW). Conditions: coagulant = $Al_2(SO_4)_3$; coagulant dosage = 0.8 g L^{-1}; pH_0 = 4.5; effluent after 1 h sedimentation and removal of coagulation sludge; [c] OMW after biological oxidation (bio-OMW). Conditions: pH = 7.3–8.3; $T = 25 \pm 5$ °C; V = 80 L; DO ≈ 2 mg L^{-1}; [d] OMW after PF-UVA process. Conditions: t = 3 h; $pH_0 = pH_{final}$ = 2.8 (controlled during reaction); $T = 25 \pm 1$ °C; $[H_2O_2]$ = 400–500 mg L^{-1}; $[TDI]_0$ = 100 mg L^{-1}; Q = 50 L h^{-1}; V = 1.1 L; 6 W UVA light source; neutralized OMW to pH = 7.0 not characterized; FluHelik photoreactor; [e] OMW after AO process. Conditions: t = 3 h; pH_0 = 8.3 (natural); $T = 25 \pm 1$ °C; j = 200 mA cm^{-2}; Q = 50 L h^{-1}; V = 1.1 L; MicroFlowCell and FluHelik photoreactor; [f] OMW after O_3 process. Conditions: t = 3 h; pH_0 = 8.3 (natural); $T = 25 \pm 5$ °C; Q_{O3} = 0.2 Ndm^3 min^{-1}; OD_I = 20 mg O_3 min^{-1}; V = 1.0 L; Bubble column reactor; [g] Emission limit values (ELV) for wastewater disposal into aquatic environment, imposed by the Portuguese legislation [26]; [h] Limit of quantification (LOQ) value; d – detected; n.a. – not applicable; n.d. – not detected; n.m. – not measured.

sludge and solids, and oil and grease.

2.3. Analytical determinations

All analytical methods employed in the present work are described in the *Supplementary Material* file (Table SM-1).

2.4. Experimental system and procedure

2.4.1. Coagulation/flocculation

The coagulation/flocculation process was conducted in batch and continuous mode (described below), assessing the effect of the pH, and the type and dosage of coagulant and flocculant. The reproducibility of the trials was verified by conducting it in duplicate. The efficiency of the treatment was evaluated as a function of chemical oxygen demand (COD), dissolved organic carbon (DOC), turbidity, and phenols removal after 30 min settling. Subsequently, the best-operating conditions were applied to 80 L of the p-OMW so that a sufficient volume of the coagulated OMW (c-OMW) could be obtained for the subsequent procedures (Table 2).

2.4.1.1. Batch mode. Batch tests were carried out in a jar-test apparatus (Velp Scientifica, Model JLT6) using 300 mL of p-OMW inside 500 mL beakers. The pH was adjusted (when applicable) in the range of 3.0–4.5. A coagulant dosage ($Al_2(SO_4)_3$: 200–3000 mg L^{-1}; Chitosan: 100–500 mg L^{-1}; $FeCl_3$: 100–500 mg L^{-1}) was added, and mechanical stirring was provided for 3 min at 150 rpm, followed by 15 min at 20 rpm. The choice of the coagulants ($Al_2(SO_4)_3$, chitosan, and $FeCl_3$) was based on its conventional use for OMW coagulation [27]. Under the best conditions, flocculation was tested using Ambifloc, Superfloc or Magnafloc flocculants in the range of 1.2–4.0 mg L^{-1} under slow stirring (20 rpm for 15 min).

2.4.1.2. Continuous mode. The best conditions established for batch were replicated in a continuous mode setup composed of (i) a feed tank with the p-OMW, (ii) a stirred tank reactor (109 mL) for coagulation, (iii) a tubular reactor (130 mL) for flocculation (if applicable), and (iv) a settling tank for clarification (Fig. SM-1a). More details can be found elsewhere [28]. The p-OMW was pumped continuously into the system, at a flow rate of 12 mL min^{-1}. After reaching steady-state conditions, the c-OMW was collected for the subsequent stages.

2.4.2. Biological oxidation

The biological system was conducted in batch mode using a 100 L cylindrical flat-bottom tank with mechanical stirring (Ingenieurbüro CAT Scientific, model R50D) and air supply, provided by an air pump (Aqua Medic, model Mistral 4000) connected to a diffuser at the bottom of the tank, under ambient temperature (25 ± 5 ºC) (Figure SM-1b). Initially, 5 L of activated sludge from a municipal wastewater treatment plant and 5 L of c-OMW (previously neutralized up to pH 7.0) were added to the tank. For 14 days, small amounts of c-OMW were progressively incorporated into the biological reactor (and DOC decrease monitored), allowing the biomass to adapt to such a complex matrix until reaching a total volume of 85 L. Following this adaptation period, the biological oxidation continued for more 20 days (0.5 g L^{-1} < volatile suspended solids (VSS) < 1.0 g L^{-1}; 7.3 < pH < 8.3; and dissolved oxygen (DO) ~0.5 mg L^{-1}) until DOC stabilization. H_2SO_4 was continuously added to keep pH in the intended range. After 24 h sedimentation, the supernatant (bio-OMW) was carefully withdrawn and used for the subsequent AOPs trials.

2.4.3. Advanced oxidation processes

After the second stage, the resulting effluent (bio-OMW) underwent three different AOPs: PF-UVA, AO, and O_3. For every trial, a total treatment time of 3 h (180 min) was applied. DOC was monitored along the various AOPs. A zero-order kinetic constant ($k_{DOC/ODT}$, mg C g O_3^{-1}) and pseudo-first-order kinetic constants for DOC removal (k_{DOC}, min^{-1}) were calculated from Eqs. (1) and (2), respectively:

$$[DOC]_t = [DOC]_0 - k_{DOC/ODT} OD_{T,t} \quad (1)$$

$$[DOC]_t = [DOC]_0 e^{-k_{DOC} t} \quad (2)$$

where $[DOC]_t$ is the DOC content (mg C L^{-1}) after time t and $[DOC]_0$ is the DOC content (mg C L^{-1}) just before the start of the reaction, and $OD_{T,t}$ (g O_3 L^{-1}) is estimated transferred dose of ozone (see Eq. (4)) after time t. The goodness of the fitting was assessed by calculating the relative standard deviations, the coefficient of determination (R^2), and the residual variance.

2.4.3.1. Photo-Fenton. PF-UVA treatment tests (Fig. SM-1c.1) were carried out in a lab-scale flow system composed by: (i) a FluHelik photoreactor (680 mL), (ii) a recirculation cylindrical glass vessel (1.5 L), thermostatically controlled and magnetically stirred, (iii) a gear pump (Ismatec, model BVP-Z), and (iv) an UVA lamp (Philips TL 6 W/08 fluorescent black light blue lamp). All system units were connected by polytetrafluoroethylene (PTFE) tubing. The FluHelik photoreactor has already been extensively described elsewhere [29]. Briefly, it is mainly composed of (i) a cylindrical stainless-steel shell, (ii) inlet/outlet pipes located perpendicularly to the fluid flow and tangentially to the shell in a horizontal plane and at the top in opposite sides, and (iii) a concentric inner quartz tube housing the lamp. The radiant power reaching the FluHelik/UVA system was 0.62 ± 0.02 W [30].

For the PF-UVA trials, a volume of 1.1 L of the bio-OMW was added to the glass vessel, the thermostatic bath was switched on, and homogenization by recirculation at 50 L h^{-1} in the dark occurred until the OMW achieved a temperature of 25 ± 1 ºC (~10 min). Then, an initial control sample was taken. A flow rate of 50 L h^{-1} was applied during all tests since good hydrodynamic conditions take place inside the FluHelik photoreactor for flow rates ≥ 50 L h^{-1} [29]. Then, the pH of the bio-OMW was adjusted to the intended value (2.8, 3.5 or 4.0) and a second control sample was collected. Afterward, the catalyst was added (40, 60, 80 or 100 mg Fe^{2+} L^{-1}) and, after 5 min of recirculation, a third control sample was obtained (t = 0 min). Finally, the lamp was turned on simultaneously with the addition of the oxidant (100–250 or 400–500 mg H_2O_2 L^{-1}), giving the reaction start. The Fenton trial (absence of light) was similarly conducted (pH = 2.8, T = 25 ± 1 ºC; $[H_2O_2]$ = 400–500 mg L^{-1}; $[TDI]_0$ = 100 mg L^{-1} and 50 L h^{-1}). The H_2O_2 was continuously added during the trials to maintain the pre-determined concentration constant during the entire reaction time. The temperature supplied by the thermostatic bath was continuously adjusted to keep the OMW at 25 ± 1 ºC. The pH was also adjusted to its initial value during reactions. Samples were collected at different time intervals. After samples collection, sodium sulfite (Na_2SO_3) was added in a Na_2SO_3-to-H_2O_2 molar ratio of 1:1 [31] to quench H_2O_2 and stop the oxidation process.

2.4.3.2. Anodic oxidation. AO system setup (Fig. SM-1c.2) was similar to the previously described for PF-UVA, but (i) coupling the FluHelik photoreactor to a conventional electrochemical filter-press flow cell (ElectroCell, model MicroFlowCell), and (ii) using an UVC lamp (Philips G11T5, 11 W, low-pressure mercury lamp) inside the photoreactor (for AO/UVC). The radiant power reaching the FluHelik/UVC system was 1.71 ± 0.03 W [29]. The electrochemical cell was equipped with (i) a boron-doped diamond (BDD) anode (active area of 10 cm^2) composed of a conductive niobium (Nb) sheet with 2 mm thickness coated with a BDD film of ~2 μm thickness, and (ii) a platinum (Pt) cathode (active area of 10 cm^2) composed of a conductive titanium (Ti) plate of 2.0 mm thickness two-side coated with a thin pure Pt film of ~2.5 μm thickness. Both electrodes were supplied by ElectroCell. A power supply (MLINK, model DPS3005, 0–5 A, 0–30 V) provided constant current density (j,

mA cm^{-2}) to the cell and directly displayed the cell potential. The characteristics of the electrochemical cell are detailed elsewhere [32].

A volume of 1.1 L of the bio-OMW (in the absence or presence of 3.0 g NaCl L^{-1}) was added to the glass vessel, the thermostatic bath was switched on, and homogenization by recirculation at 50 L h^{-1} in the dark occurred until the OMW achieved a temperature of 25 ± 1 °C (~10 min). An initial control sample was taken. The beginning of the AO process was marked by the switch of the power supply at a constant *j* (25, 100, 150 or 200 mA cm^{-2}) and, for the AO/UVC process, by the simultaneous switch of the UVC light. The temperature supplied by the thermostatic bath was continuously adjusted to keep the OMW at 25 ± 1 °C. The pH was measured but not adjusted during reactions. Samples were collected at different time intervals. The energy consumption for the operation of the electrochemical cell was calculated in terms of specific energy consumption per unit volume (EC, kWh m^{-3}) according to Eq. (3) [33]:

$$EC = \frac{E_{cell} I\, t}{V_s} \quad (3)$$

where E_{cell} is the average cell voltage (V), I is the current intensity (A), t is the time of reaction (h), and V_s is the volume of solution (L).

2.4.3.3. Ozonation. The lab-scale setup for O_3 trials (Fig. SM-1c.3) mainly encompassed: (i) an ozone generator (BMT, model 802 N, gas flow range 0.1–1.0 Ndm^3 min^{-1}) fed by pure/dry oxygen at a constant flow rate regulated by a digital mass flow controller (Alicat Scientific, MC-Series model with standard accuracy of ± 0.6%), (ii) a bubble column (BC) (BMT, model 4.1) (73 mm of internal diameter, 370 mm of maximum column height, and ~1.5 L volume capacity) without bio-OMW recirculation, (iii) a porous ceramic diffuser, placed at the bottom of the BC, through which a constant flow of an ozone/oxygen-gas mixture was being delivered, and (iv) an UV-based ozone analyzer (BMT, model 964) coupled to a dehumidifier (BMT, model DH3b) to monitor inlet and outlet gaseous ozone concentrations. The residual ozone gas was vented through a catalytic destruction unit (BMT, Heated Catalyst) and bubbled into Woulff bottles containing 2% potassium iodide solution. All system units were connected by PTFE tubing. The system was placed inside a fume cupboard to avoid exposure to ozone. More information on this system can be accessed in Gomes, *et al.* [34].

For O_3 trials, a volume of 1 L of the bio-OMW was added to the BC, and different inlet ozone doses (OD_I = 12, 20 or 40 mg O_3 min^{-1}) were tested by increasing the inlet concentration of ozone ($C_{O3,I}$ = 60, 100 or 200 mg Ndm^{-3}) under a constant gas flow rate (Q_g = 0.2 Ndm^3 min^{-1}). During 3 h of treatment time, periodic samples were collected for analytical characterization. Before the analysis, dissolved ozone was removed by transferring the sample vials into a water bath at 50 °C for 15 min. Temperature and pH were not controlled during reactions. The ozone consumption was evaluated through the mass balance of ozone in the gas phase as a function of the estimated transferred dose of ozone (OD_T, g O_3 L^{-1}), following Eq. (4) [34]:

$$OD_T = \frac{Q_g}{V_L}\int_0^t (C_{O3,I} - C_{O3,O})\,dt \quad (4)$$

where Q_g is the applied gas flow rate (Ndm^3 min^{-1}), V_L is the OMW volume in the column (L), and $C_{O3,I}$ and $C_{O3,O}$ are the inlet and the outlet/off-gas ozone concentration in the gas phase (g O_3 Ndm^{-3}), respectively, during the applied time interval (*t*, min).

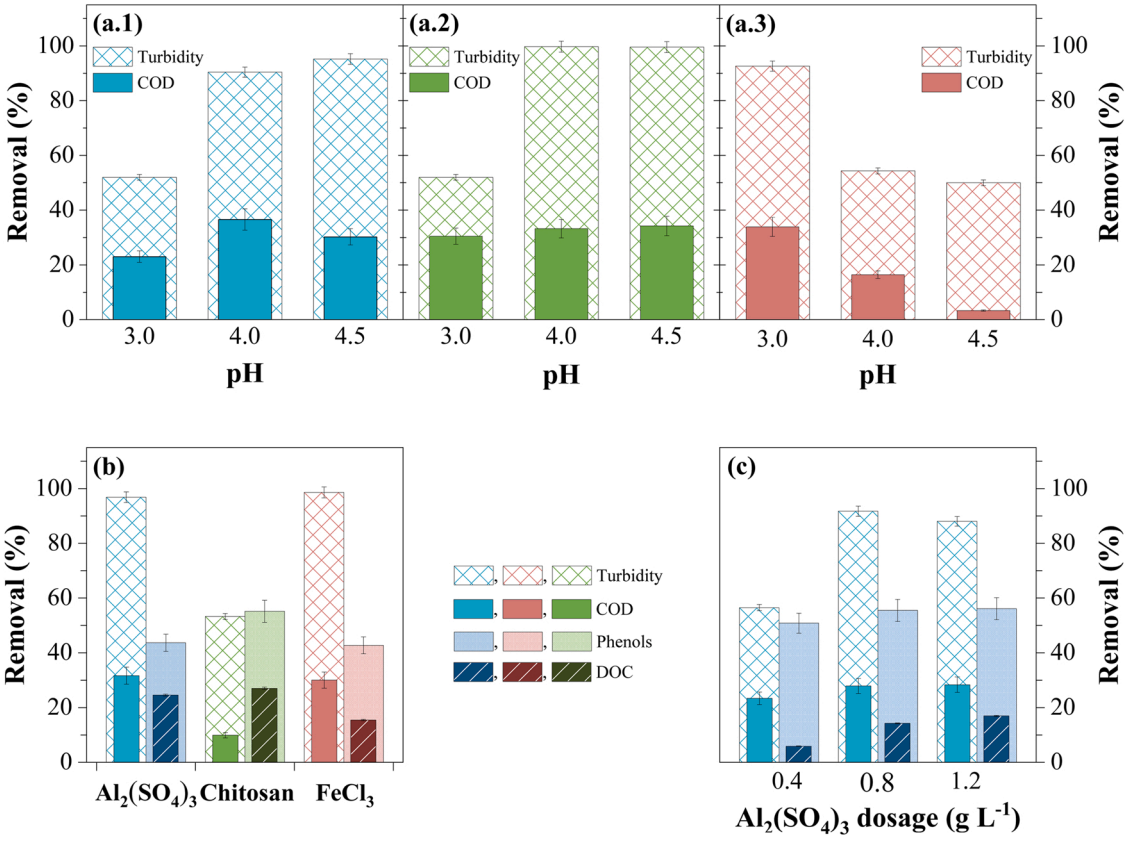

Fig. 1. Performance of coagulation process for (a) batch mode tests aiming pH selection using different coagulants at fixed dosages – (a.1) $Al_2(SO_4)_3$ = 0.4 g L^{-1}, (a.2) chitosan = 0.1 g L^{-1}, and (a.3) $FeCl_3$ = 0.1 g L^{-1}, (b) batch mode tests aiming coagulant selection using the best pH for each coagulant (pH = 4.5 for $Al_2(SO_4)_3$, pH = 4.5 for chitosan, and pH = 3.0 for $FeCl_3$) and dosage = 0.5 g L^{-1}, and (c) continuous mode aiming coagulant dosage selection using $Al_2(SO_4)_3$ and pH = 4.5. Absence of flocculant addition in all trials. Error bars represent the range of results from duplicate trials.

3. Results and discussion

3.1. Olive mill wastewater characteristics

The r-OMW (not physicochemically characterized due to constraints provided by the high amount of sludge and solids, and oil and grease) had a strong olive smell and a dark brown color. After the filtration/sedimentation pre-treatment for removal of larger particles and oil and grease (p-OMW), it showed (i) a high concentration of organic compounds (COD of ~10 g O_2 L^{-1} and DOC of ~2.9 g C L^{-1}), (ii) a high content of particulate matter (TSS of ~4 g L^{-1} and turbidity of 4600 NTU), (iii) the presence of phenol compounds (161 mg L^{-1}), and (iv) an acidic pH (~4.5) (Table 2).

Even though biological methods are commonly used to pre-treat/treat OMWs [7, 35–37], it is a common practice to dilute the OMW prior to the biological treatment to decrease the negative effect of high organic loads, including phenolic compounds, on microbial activity [7, 23,35,38]. This occurs because it is well known that microorganisms can be highly inhibited by the presence of phenolic compounds [5,23,37]. The 28-day Zahn-Wellens biodegradability test (Fig. SM-2, Table 2) confirmed the need for a 10-time dilution for the p-OMW to attain a biodegradation ≥ 70%, so that the application of a biological oxidation stage can be considered viable. In this sense, the application of an AOP to increase p-OMW biodegradability could be an option, but the expected operating costs at this point would be extremely high. Furthermore, photocatalytic processes would be undermined by the high turbidity and color of the p-OMW. Considering that the aim is to provide a treatment strategy with no need for wastewater dilution and economically feasible, a coagulation/flocculation process was chosen to be tested as the first treatment stage.

3.2. First-stage - coagulation/flocculation

3.2.1. Batch mode

Coagulation of OMWs is recognized to enable substantial solids removal, organic matter, phenols content, and color, which can potentially benefit subsequent treatment stages [21,39]. The present study focused on working with minimal/null pH adjustment. Taking this into consideration, pH optimization tests were performed at the natural pH of the p-OMW or pH values close to it (pH 3.0–4.5), using the minimum coagulant dosage that provided a visible agglomeration of particles (0.4 g L^{-1} for $Al_2(SO_4)_3$, and 0.1 g L^{-1} for chitosan and $FeCl_3$) (Fig. 1a). For $Al_2(SO_4)_3$, COD and turbidity removal decreased for lower pH values, achieving the best results at natural pH (Fig. 1a.1–2). At pH 4.5, $Al_2(SO_4)_3$ could be causing a dual effect: (i) the soluble complexes coming from humic substances were more easily generated in the presence of Al^{3+}, and (ii) the aluminum hydroxide species formed (Al $(OH)_3$) increased the adsorption of humic acids on its surface [40]. For chitosan, changing the p-OMW pH did not influence the coagulation efficiency (Fig. 1a.2). Chitosan is a positively charged linear polyelectrolyte under acidic conditions (pH ~4), and its amine functional groups attract anionic ions (such as those present in the OMW humic acids), which improves its adsorption and coagulation effects [41]. Conversely, decreasing the p-OMW pH improved COD and turbidity removal when $FeCl_3$ was used as a coagulant (Fig. 1.a.3). At lower pH values (~3), the predominant ferric ions are in the hydrated aquo state, so the destabilization mechanism is mainly due to the ionic strength. At pH > 4.5, the hydrolyzation of the ferric ions leads to the precipitation of the ferric hydroxide, which is insoluble [42].

For each coagulant, under the respective best pH (pH 4.5 for $Al_2(SO_4)_3$ and chitosan, and pH 3.0 for $FeCl_3$), the same dosage (0.5 g L^{-1}) was then applied (Fig. 1b). The results for $Al_2(SO_4)_3$ and $FeCl_3$ were quite similar and showed the superiority of these coagulants over chitosan in decreasing both COD (~30% *vs.* 10%) and turbidity (~98% *vs.* 53%). Despite this, chitosan provided a slightly higher phenols (~44% *vs.* 55%) and DOC (~20% *vs.* 27%) removal. Further jar-tests with the addition of different types and dosages of flocculants showed null improvement (data not shown). These results indicate $Al_2(SO_4)_3$ as the best coagulant choice since (i) higher efficiencies were obtained (*vs.* chitosan), and (ii) no pH adjustment was required (*vs.* $FeCl_3$). It should be noted that if a subsequent Fenton's reaction-based treatment stage is expected, then it makes sense to choose the $FeCl_3$ coagulant. Not only does this coagulant work best at pH 3.0 (usually the optimum pH value for Fenton's reaction-based processes), but the remaining iron can reduce the amount of catalyst to be added if this AOP treatment follows.

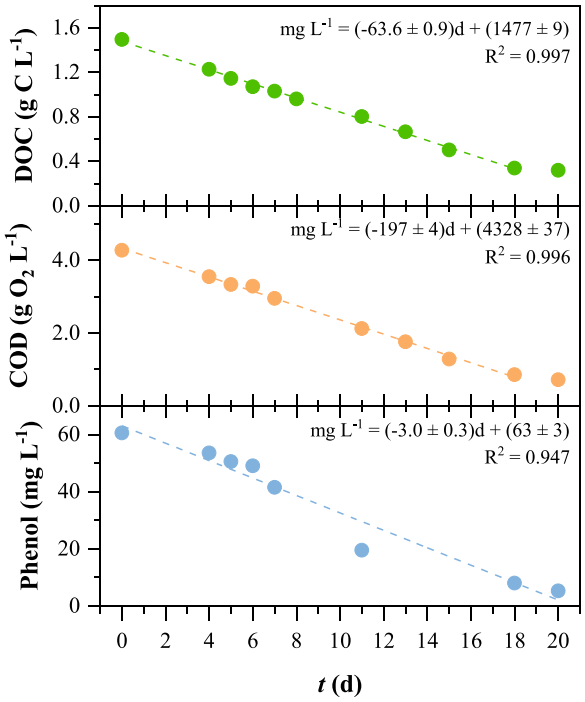

Fig. 2. Evolution of DOC ( ), COD ( ) and phenol ( ) concentrations during the biological oxidation process. Conditions: pH = 7.3–8.3; T = 25 ± 5 °C; V = 80 L; DO ≈ 2 mg L^{-1}.

3.2.2. Continuous mode

Coagulation of the p-OMW in continuous mode using different dosages of $Al_2(SO_4)_3$ and at natural pH provided lower efficiencies (Fig. 1c) compared to the batch operation, as jar-test operates under optimum mixture conditions. For $Al_2(SO_4)_3$ dosages of 0.8 g L^{-1} and 1.2 g L^{-1}, similar removal efficiencies were obtained for the studied parameters and overall better results compared with those achieved for 0.4 g L^{-1}. Once again, the addition of flocculant showed null process improvement compared with coagulation alone (data not shown). These results established the dosage of 0.8 g L^{-1} of $Al_2(SO_4)_3$ at pH = 4.5 (null pH adjustment) as the best coagulation conditions for the p-OMW.

Coagulation, as the first treatment stage, was able to decrease TSS by 97%, turbidity by 98%, phenol compounds by 57%, and the organic matter content by 20% for COD and 17% for DOC (Table 2). This led to a decrease in the inhibition on the biological activity and the resulting c-OMW reached a mineralization of 88 ± 2% with 1:2 and 1:10 dilution at the end of the 28-day Zahn-Wellens test (Fig. SM-2, Table 2), thus indicating the increase in the biodegradability of the c-OMW and that biological oxidation could be applied in the subsequent treatment stage.

For an OMW also coagulated with $Al_2(SO_4)_3$, Achak, *et al.* [27] reported higher DOC removal (38 ± 5%) when applying coagulant dosages of 1.5–1.9 g L^{-1}. In turn, under quite similar experimental conditions (pH = 4.6 and $Al_2(SO_4)_3$ = 0.8 g L^{-1}), Vuppala, *et al.* [43] found comparable reductions of 17% for DOC, 57% for COD, 62% for phenols and 93% for turbidity (OMW initial conditions: DOC =

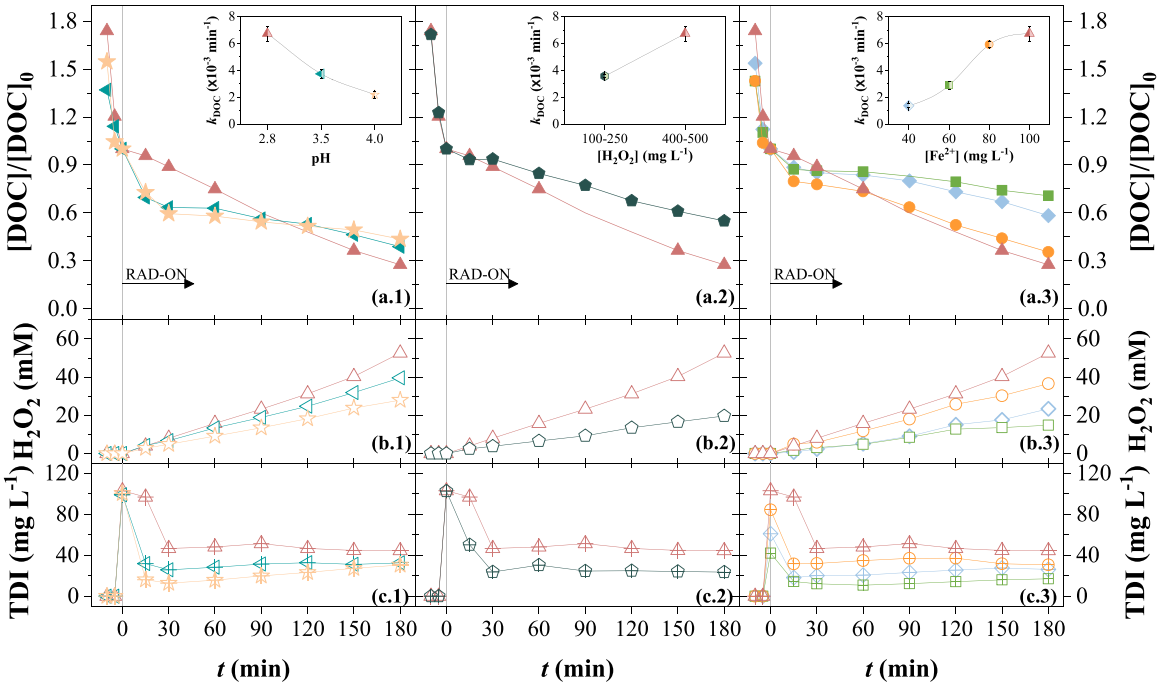

Fig. 3. Evolution of the (a) normalized DOC removal (inset: respective pseudo-first-order kinetic constants), (b) H_2O_2 consumption, and (c) total dissolved iron (TDI) concentrations as a function of reaction time during the PF-UVA reactions for different (.1) pH values ((▲,△,⊞) – pH = 2.8; (◀,◁,⊕) – pH = 3.5; (★,☆,✳) – pH = 4.0), (.2) H_2O_2 concentrations ((⬟,⬠,⊕) – [H_2O_2] = 100-250 mg L^{-1}; (▲,△,⊞) – [H_2O_2] = 400-500 mg L^{-1}), and (.3) Fe^{2+} initial concentrations ((■,□,⊞) – $[TDI]_0$ = 40 mg L^{-1}; (◆,◇,⊕) – $[TDI]_0$ = 60 mg L^{-1}; (●,○,⊕) – $[TDI]_0$ = 80 mg L^{-1}; (▲,△,⊞) – $[TDI]_0$ = 100 mg L^{-1}). Conditions: (.1) – [H_2O_2] = 400-500 mg L^{-1}, $[TDI]_0$ = 100 mg L^{-1}; (.2) – pH = 2.8, $[TDI]_0$ = 100 mg L^{-1}; (.3) – pH = 2.8, [H_2O_2] = 400-500 mg L^{-1}; (for all) – T = 25±1 °C; Q = 50 L h^{-1}; V = 1.1 L; 6 W UVA light source; FluHelik photoreactor.

2.6 g C L^{-1}, COD = 16.4 g O_2 L^{-1}, phenols = 159 mg L^{-1}).

3.3. Second stage – biological oxidation

Biological oxidation lasted 20 days, during which low levels of DO (~0.5 mg L^{-1}) were indicative of a high degree of oxidation (data not shown). Towards the end of the biological treatment, along with DOC stabilization (Fig. 2), DO contents started to increase up to 2.0 mg L^{-1} and over, suggesting that the biodegradable compounds were already oxidized. The biological process provided a continuous DOC, COD and phenols decay (Fig. 2), with average rates of 63.6 ± 0.9 mg L^{-1} d^{-1} (R^2 = 0.997), 197 ± 4 mg L^{-1} d^{-1} (R^2 = 0.996), and 3.0 ± 0.3 mg L^{-1} d^{-1} (R^2 = 0.947), respectively. As a result, the biological stage provided almost complete phenols removal (92%), along with the oxidation of almost all biodegradable organic compounds (removal of 89 ± 2% of organic matter), as can be seen in Table 2. These reductions are related to the microorganisms' strong activity to use organic matter and phenol-like compounds as carbon and energy sources [44,45]. This is only possible due to an acclimatization period [46], which lasted for 14-days in this study. Part of the removal of phenols verified at this stage may also be related to the volatilization of some phenolic compounds due to the air injection supplied during treatment. Even though biological treatments based on activated sludge do not provide high removal on the organic load of OMWs [11,39], the combination of biological oxidation with other treatment processes can significantly improve pollutants removal [2,35,37], as proven in this work.

3.4. Third stage – advanced oxidation processes

3.4.1. Photo-Fenton

The most well studied AOPs in the treatment of OMWs are Fenton and PF [11,13,14,21,23]. PF is based on the Fenton's reaction (Eq. (5)) [47]) coupled with radiation (Eq. (6)) [48], which results in higher production of $HO^{\bullet}$ [15,21] and, ultimately, higher efficiencies.

$$Fe^{2+} + H_2O_2 \rightarrow Fe^{3+} + HO^{\bullet} + HO^{-} \quad (5)$$

$$Fe^{3+} + H_2O + h\nu \rightarrow Fe^{2+} + HO^{\bullet} + H^{+} \quad (6)$$

A Fenton process was firstly applied during 3 h, which promoted a very poor organics degradation (data not shown).

PF-UVA tests were carried out using the bio-OMW acidified at pH values of 2.8, 3.5, and 4.0 (Fig. 3a-c.1, Table SM-2). It must be mentioned that the preliminary acidification step led to a decrease of the organic matter content (average DOC reduction of 26 ± 4%), which was probably related to the precipitation of humic acids/phenolic compounds [49]. For the PF-UVA treatment acidified up to pH 2.8, continuous removal of DOC was observed throughout the reaction, achieving a reduction of 72% at the end (Fig. 3a.1). Photo-treatments at pH 3.5 and 4.0 presented sharp mineralization (~30%) between $0 < t < 15$ min, followed by a very slight DOC abatement period (~30%) towards the end. This trend can be mainly related to high Fe^{3+} precipitation at the beginning of the reaction, $0 < t < 15$ min, as indicated by the total dissolved iron (TDI) concentration profiles (Fig. 3 c.1). For pH > 2.8 the generated Fe^{3+} may have precipitated along with the organic compounds with which it formed complexes.

The optimization of H_2O_2 concentration can minimize H_2O_2 consumption and improve the reaction rate·H_2O_2 can be rate-limiting if applied in too low concentrations, leading to a reduction of the Fenton's reaction (Eq. (5)) [19,22], and it also participates in parasitic reaction (Eq. (7) [50]), or it can self-decompose (Eq. (8)) [51] if applied at too high concentrations. For the same catalyst concentration (100 mg Fe^{2+} L^{-1}), two oxidant dosages were evaluated by initially adding (i) 250 mg L^{-1} of H_2O_2 and maintaining the dosage between 100 and 250 mg L^{-1} (H_2O_2/Fe^{2+} molar ratio = 4), or (ii) 500 mg L^{-1} of H_2O_2,

keeping a range dosage of 400–500 mg L^{-1} (H_2O_2/Fe^{2+} molar ratio = 9). This stepwise addition of H_2O_2 has been shown to improve the efficiency of the Fenton process on the treatment of an OMW compared to the single-dose method [5]. The obtained results (Fig. 3a-c.2, Table SM-2) indicate that increasing the oxidant concentration benefited the process by increasing DOC removal (k_{DOC} increase of 1.9-fold), although with a slightly higher H_2O_2 consumption (Fig. 3b.2). A further increase in oxidant concentration is expected to lead to the occurrence of scavenging/parasitic reactions (Eqs. (7) and (8)) [50,51].

$$H_2O_2 + HO^{\bullet} \rightarrow HO_2^{\bullet} + H_2O \quad (7)$$

$$2H_2O_2 \rightarrow O_2 + H_2O \quad (8)$$

The increase of the catalyst concentration (Fig. 3a-c.3) led to higher and faster organic matter removal due to greater production of $HO^{\bullet}$ via Eq. (5). Moreover, a low H_2O_2 consumption rate associated with an induction period ($0 < t < 30$ min) occurred for the tests using the lowest iron concentrations. This suggests that after the initial H_2O_2 addition and subsequent Fe^{2+} oxidation, the rate-limiting step of the reaction is described by Eq. (6) as a result of photonic competition between the iron complexes and other light-absorbing species. The competition decreases as Fe^{2+} concentration increases, being almost null for the highest concentration tested (100 mg Fe^{2+} L^{-1} with H_2O_2/Fe^{2+} molar ratio = 9). It should be noted that the reaction rate of mineralization (see Table SM-2) doubles when the catalyst dosage increases from 40 to 60 mg Fe^{2+} L^{-1} and again from 60 to 80 mg L^{-1}, while it has only a small increase (~14%) from 80 to 100 mg Fe^{2+} L^{-1}. Taking this, and considering that further increase in Fe^{2+} concentration can also have scavenging effects (Eq. (9)) [52], higher catalyst dosages were not pursuit.

$$Fe^{2+} + HO^{\bullet} \rightarrow Fe^{3+} + HO^{-} \quad (9)$$

Considering that the best performance of the PF-UVA process was attained with a pH 2.8, keeping the oxidant in the range of 400–500 mg H_2O_2 L^{-1}, and a catalyst dosage of 100 mg Fe^{2+} L^{-1}, these were defined as the best operational conditions for the treatment of the bio-OMW.

3.4.2. Anodic oxidation

AO is a clean alternative since it resorts to electrons (e^-) as reagents. In AO with non-active anodes as BDD, organics can be oxidized by three main mechanisms: (i) the direct transfer of e^- from the organics *R* to the anode surface via Eq. (10) [53], (ii) the attack of heterogeneous reactive species produced as intermediates of water oxidation, including (1) powerful physisorbed $HO^{\bullet}$ at the anode surface, denoted $M(HO^{\bullet})$, generated via Eq. (11) [53], (2) H_2O_2 produced from $M(HO^{\bullet})$ dimerization according to Eq. (12) [53], and (3) O_3 generated from water discharge at the anode surface via Eq. (13) [53], and/or (iii) oxidants that are electrochemically produced from species existing in the bulk solution, such as active chlorine species (chlorine – Cl_2, hypochlorous acid – HClO, and hypochlorite ion – ClO^-) generated from chloride ions (Cl^-) via Eqs. (14)-(16) [53,54], persulfate ($S_2O_8^{2-}$) formed from sulfate ions (SO_4^{2-}) via Eq. (17) [53], and sulfate radicals ($SO_4^{\bullet-}$) able to be produced by various pathways, such as SO_4^{2-} oxidation at the anode surface via Eq. (18) [55], $S_2O_8^{2-}$ reaction with $HO^{\bullet}$ or an organic R via Eqs. (19) or (20) [56], and $S_2O_8^{2-}$ cathodic reaction via Eq. (21) [57].

$$R \rightarrow (R^{\bullet})^{+} + e^- \quad (10)$$

$$M + H_2O \rightarrow M(HO^{\bullet}) + H^+ + e^- \quad (11)$$

$$2M(HO^{\bullet}) \rightarrow 2MO + H_2O_2 \quad (12)$$

$$3H_2O \rightarrow O_3 + 6H^+ + 6e^- \quad (13)$$

$$2Cl^- \rightarrow Cl_2 + 2e^- \quad (14)$$

$$Cl_2 + H_2OH \rightleftharpoons ClO + Cl^- + H^+ \quad (15)$$

$$HClO \rightleftharpoons ClO^- + H^+ \quad (16)$$

$$2SO_4^{2-} \rightarrow S_2O_8^{2-} + 2e^- \quad (17)$$

$$SO_4^{2-} \rightarrow SO_4^{\bullet-} + e^- \quad (18)$$

$$S_2O_8^{2-} + HO^{\bullet} \rightarrow HSO_4^- + SO_4^{\bullet-} + \frac{1}{2}O_2 \quad (19)$$

$$S_2O_8^{2-} + R \rightarrow 2SO_4^{\bullet-} + (R^{\bullet}) \quad (20)$$

$$S_2O_8^{2-} + e^- \rightarrow SO_4^{2-} + SO_4^{\bullet-} \quad (21)$$

Fig. 4a shows that the increase of the *j* (from 25 to 200 mA cm^{-2}) provided sharper DOC removals as a function of reaction time. This can be attributed to the occurrence in a greater extent of the direct e^- transfer from the organics to the anode via Eq. (10) and/or the production of higher amounts of oxidative species, such as $M(HO^{\bullet})$, H_2O_2, O_3, active chlorine species, $S_2O_8^{2-}$ and/or $SO_4^{\bullet-}$ via Eqs. (11)–(21) that may attack the bio-OMW organics and/or the organic by-products generated during the AO process. The generation of active chlorine species was confirmed during reactions (Table SM-3). After 3 h of electrolysis at 200 mA cm^{-2}, active chlorine species reached a content of 114 mg L^{-1}. DOC removals of 15%, 21%, 26%, and 30% were obtained at the end of AO trials using 25, 100, 150, and 200 mA cm^{-2} (Table SM-3), respectively. Panizza and Cerisola [18] also achieved

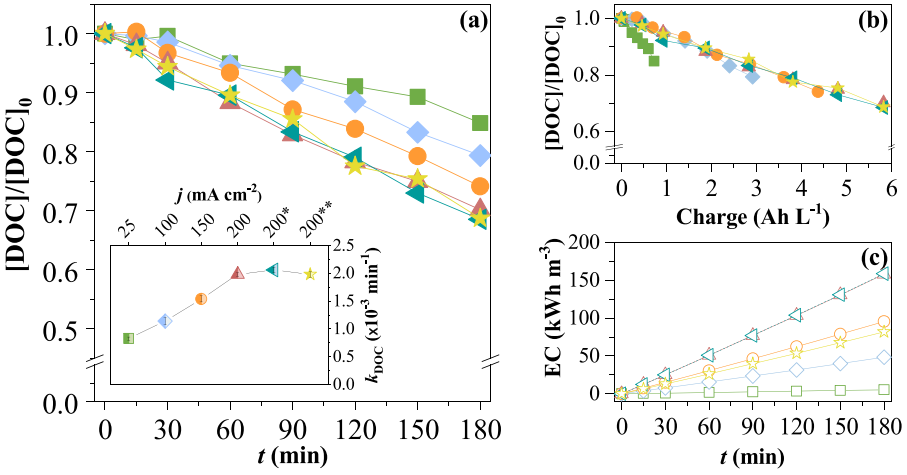

Fig. 4. Evolution of the (a) normalized DOC removal as a function of reaction time (inset: respective pseudo-first-order kinetic constants), (b) normalized DOC removal as a function of consumed charge, and (c) energy consumption for the electrolysis as a function of reaction time during the AO reactions for different current densities ((■,□) – j = 25 mA cm^{-2}; (◆,◇) – j = 100 mA cm^{-2}; (●,○) – j = 150 mA cm^{-2}; (▲,△) – j = 200 mA cm^{-2}), and for j = 200 mA cm^{-2} (◀,◁) in the presence of 11 W UVC light source and (★,☆) in the presence of 3.0 g L^{-1} of NaCl. Conditions: pH_0 = 8.3 (natural); T = 25 ± 1 °C; Q = 50 L h^{-1}; V = 1.1 L; MicroFlowCell and FluHelik photoreactor.

increasing removal of organics (COD removal from ~10% to ~48%) for raising j from 37 to 62 mA cm^{-2} in a 3 h AO treatment with a $TiRuO_2$ anode applied to a filtered OMW with a much higher COD (26, 750 mg O_2 L^{-1} *vs.* 718 mg O_2 L^{-1}).

Fig. 4b shows the DOC decay profiles in terms of consumed charge for the electrolysis. The behavior was distinct from that in terms of electrolysis time. For the same specific charge, the DOC was removed to a greater extent for 25 mA cm^{-2} and poorly and similarly removed for 100–200 mA cm^{-2}, suggesting a beneficial effect of a low j of 25 mA cm^{-2}, and the absence of adverse effects of applying $j > 100$ mA cm^{-2}. After a consumed charge of 5.8 Ah L^{-1} using 200 mA cm^{-2}, 30% of DOC removal was achieved. Chatzisymeon, *et al.* [58] achieved 10% COD removal after a consumed charge of ~6 Ah L^{-1} using 86 mA cm^{-2} in the AO treatment with a BDD anode of a filtered and highly biodegradable OMW with a much larger content of organics (COD of 40 g O_2 L^{-1}). Regarding the energy consumption for the electrolysis, the application of larger j was always highly detrimental (Fig. 4c).

To further improve the efficiency of the AO, the process was assisted by UVC light. This UV radiation may decompose some electrogenerated by-products (such as H_2O_2, O_3, $S_2O_8^{2-}$ and HClO) into powerful oxidants ($HO^{\bullet}$, $SO_4^{\bullet-}$ and chlorine radical ($Cl^{\bullet}$)), according to Eq. (22) [59], (23) [60], (24) [61] and (25) [62]. Furthermore, despite the inability of the original organics of the bio-OMW to UVC photolysis (data not shown), some AO by-products can be susceptible to the attack of UVC radiation. Ultimately, this can lead to better oxidation of organics.

$$H_2O_2 + h\nu \rightarrow 2HO^{\bullet} \quad (22)$$

$$O_3 + H_2O + h\nu \rightarrow 2HO^{\bullet} + O_2 \quad (23)$$

$$S_2O_8^{2-} + h\nu \rightarrow 2SO_4^{\bullet-} \quad (24)$$

$$HClO + h\nu \rightarrow HO^{\bullet} + Cl^{\bullet} \quad (25)$$

Fig. 4 shows that there was no change in the AO efficiency with the addition of UVC light. Four plausible hypotheses for these results are that (i) the photolysis of H_2O_2, O_3, $S_2O_8^{2-}$ and HClO was incapable of occurring because UVC light did not penetrate the effluent in virtue of its dark color, (ii) H_2O_2, O_3, and $S_2O_8^{2-}$ species were not produced at all or very poorly produced, being then unable to generate powerful oxidants, (iii) $Cl^{\bullet}$ produced from HClO was not able to degrade the organics of the bio-OMW, and/or (iv) organic by-products were not susceptible to the action of UVC light.

In another attempt to enhance the efficiency of AO, Cl^- ion was added to the reaction medium through NaCl salt to improve the production of active chlorine species via Eqs. (14)-(16) and also the ions conduction. The content of Cl^- of the effluent was increased from ~0.6 g L^{-1} to ~2.4 g L^{-1}. This is a common approach in the treatment of effluents [63]. In Fig. 4, one can perceive a null improvement on the DOC removal in the presence of a higher Cl^- content, which points to a low susceptibility of the organics present in the bio-OMW to be oxidized by active chlorine species, despite the confirmation of the presence of these species in higher amount – after 3 h of electrolysis, the amount of active chlorine species was 114 mg L^{-1} in the absence of NaCl addition and 376 mg L^{-1} upon the salt addition (Table SM-3). This points to a crucial role of organics oxidation by AO played by electrogenerated M ($HO^{\bullet}$). The increase in the OMW conductivity highly reduced the cell potential, ultimately providing an energy consumption ~50% lower than that in the absence of NaCl addition (Fig. 4b).

3.4.3. Ozonation

Apart from H_2O_2 ($E^0 = 1.78$ V *vs.* standard hydrogen reduction potential (SHE)) and $HO^{\bullet}$ ($E^0 = 2.73$ V *vs.* SHE), ozone has one of the highest reducing potentials ($E^0 = 2.07$ V *vs.* SHE), being highly effective for phenolic and organic compounds removal and decolorization [64–66]. In the O_3 process, two oxidation pathways can occur: (i) organics direct reaction with ozone, which is selective and relatively slow, and (ii) organics indirect reaction through secondary oxidizers, in particular $HO^{\bullet}$, generated by ozone decomposition (reactions described from Eqs. (26)-(36) [34,67]), presenting a non-selective attack and having faster oxidation rates. While under acidic pH conditions, the direct oxidation reactions prevail, under alkaline conditions ozone easily decomposes into $HO^{\bullet}$, and the indirect oxidation pathway predominates, boosting the degradation of contaminants [17,34,39,67,68].

$$O_3 + HO^- \rightarrow HO_2^- + O_2 \quad (26)$$

$$HO_2^- + O_3 \rightarrow O_3^{\bullet-} + HO_2^{\bullet} \quad (27)$$

$$HO_2^{\bullet} \rightleftharpoons O_2^{\bullet-} + H^+ \quad (28)$$

$$O_2^{\bullet-} + O_3 \rightarrow O_3^{\bullet-} + O_2 \quad (29)$$

$$O_3^{\bullet-} + H_2O \rightarrow HO^{\bullet} + O_2 + HO^- \quad (30)$$

$$O_3^{\bullet-} + HO^{\bullet} \rightarrow HO_2^{\bullet} + O_2^{\bullet-} \quad (31)$$

$$O_3^{\bullet-} + HO^{\bullet} \rightarrow O_3 + HO^- \quad (32)$$

$$HO^{\bullet} + O_3 \rightarrow HO_2^{\bullet} + O_2 \quad (33)$$

$$H_2O_2 \rightleftharpoons HO_2^- + H^+ \quad (34)$$

$$H_2O_2 + HO^{\bullet} \rightarrow HO_2^{\bullet} + H_2O \quad (35)$$

$$HO_2^- + HO^{\bullet} \rightarrow HO_2^{\bullet} + HO^- \quad (36)$$

Taking the above, and considering the bio-OMW pH value of ~8–8.3, no pH adjustment was used on the O_3 treatment and the process was evaluated for increasing OD_I (in this case, by increasing $C_{O3,I}$) which is an important parameter because it rules not only ozonation efficiency but also its associated costs [69]. Results showed (Fig. 5a-b) a significant increase in the effluent mineralization when OD_I increased from 12 to 20 mg O_3 min^{-1} (or $C_{O3,I}$ from 60 to 100 mg O_3 L^{-1}), but the DOC removal was maintained (62% *vs.* 60%) when OD_I increased to 40 mg O_3 min^{-1} ($C_{O3,I}$ of 200 mg O_3 Ndm^{-3}). A similar trend was also verified for COD abatement (77% *vs.* 79%, Table SM-4). Although some authors reported lower organic matter removal using O_3 process [24,68], the OMW on those studies presented a higher initial organic load (at least 10 times in terms of COD), which may lead to the formation of intermediary compounds (mainly carboxylic acids, such as formic and oxalic acids) that are not oxidized and accumulate in the system [17]. Comparatively, when Karageorgos, *et al.* [70] also treated in a bubble column reactor a diluted OMW (initial COD of 1100 mg O_2 L^{-1} and pH 6.7), they had a final COD reduction of ~20% and 60% after 4 h of O_3 with $C_{O3,I}$ of 22 mg O_3 Ndm^{-3} and 60 mg O_3 Ndm^{-3}, respectively. Another critical parameter to consider is the OD_T (Fig. 5a: inset), which presented a maximum ozone utilization rate of 68% (on average). This indicates that only a fraction of the fed ozone is being consumed to degrade the OMW. Similar findings were obtained by Cañizares, *et al.* [17], with a minimum of 40% O_3 being lost. According to the results, it is also noteworthy that DOC was less efficiently removed for OD_T values greater than 1.5 g O_3 L^{-1} (Fig. 5c), which occurred for the highest OD_I tested in this work.

Considering that the bio-OMW basic pH value promotes O_3 decomposition to produce $HO^{\bullet}$ (reaction chain started by Eq. (26)), one must still consider the occurrence of direct oxidation by molecular O_3, that has high selectivity towards compounds containing aromatic rings and double bonds (such as phenolic compounds). In this case, after 3 h of O_3 process with 20 mg O_3 min^{-1}, the removal of phenols was 91%, which is in agreement with high phenols degradation reported by other researchers [16,24,69,70]. For the treatment of undiluted OMW previously coagulated and bio-treated, the optimized OD_I for the ozonation

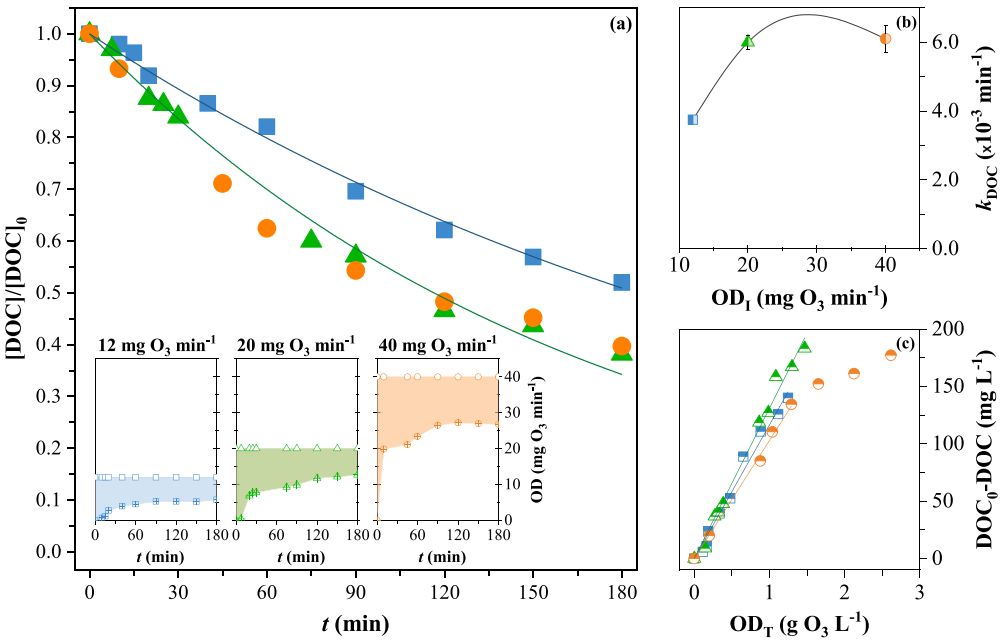

Fig. 5. Evolution of the (a) normalized DOC removal as a function of reaction time (symbols), along with the respective pseudo-first-order fitting curves (lines), (b) pseudo-first-order kinetic constants for each inlet O_3 dose (OD_I) tested, and (c) total DOC removed as a function of the transferred O_3 dose (OD_T), along with the respective zero-order fitting curves (lines) during the O_3 reactions for different OD_I (■,□,⊞,◧,◨) – 12 mg O_3 min^{-1}; (▲,△,⧋,◭,◬) – 20 mg O_3 min^{-1}; (●,○,⊕,◐,◓) – 40 mg O_3 min^{-1}). Inset: representation of the OD_I (empty symbols) and OD_O (crossed symbols) over time. The area under OD_I correspond to the total amount of O_3 available for the reaction, and the shaded area corresponds to the OD_T. Conditions: pH_0 = 8.3 (natural); $T = 25 \pm 5$ °C; $Q_{O3} = 0.2$ Ndm^3 min^{-1}; OD_I = 100 mg Ndm^{-3}; V = 1.0 L; Bubble column reactor.

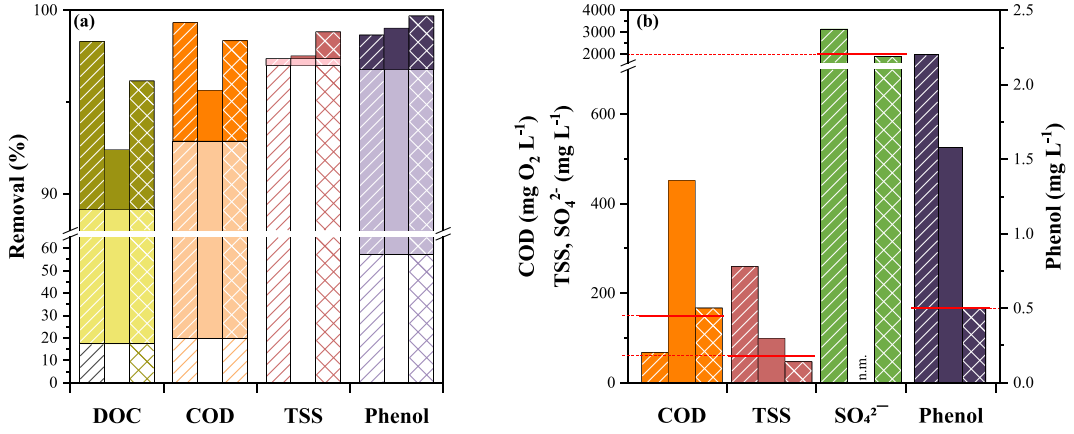

Fig. 6. Summary of the multistage treatment strategy composed of pre-treatment-coagulation-biological oxidation-AOP for (a) the overall removal of DOC, COD, TSS, and phenol, and (b) the imposed emission limit values (ELVs). The red lines in (b) represent the ELVs in Table 2. Legend: white bars – coagulation stage; light-colored bars – biological oxidation stage; dark-colored bars – AOP stage; ▨ - PF-UVA; ■ - AO; ⊠ - O_3; n.m. – not measured. Similar conditions as in Table 2.

stage (without requiring initial or final pH correction) was 20 mg O_3 min^{-1} ($C_{O3,I}$ = 100 mg Ndm^{-3} and Q_g = 0.2 Ndm^3 min^{-1}).

3.5. Multistage treatment strategy assessment

3.5.1. Removal efficiencies and legal compliance

A summary of the results for the treatment of undiluted OMW by applying a multistage strategy comprising pre-treatment (filtration and sedimentation)-coagulation-biological oxidation-AOP is presented in Fig. 6 and Table 2, considering the best operating conditions established for each tested AOP. The imposed ELVs were considered for direct discharge into environmental compartments according to the Portuguese legislation [26].

Coagulation in the first treatment stage, under the best conditions established ($Al_2(SO_4)_3$ = 0.8 g L^{-1} at pH 4.5, meaning null pH adjustment), was highly efficient in decreasing turbidity (by 98%), TSS (by 97%), and, to a lesser extent, phenols (by 57%) (Fig. 6a and Table 2). Despite the low DOC and COD removal (17% and 20%, respectively), the decrease in the inhibition on the biological activity after coagulation allowed a following biological oxidation treatment stage that further degraded the organic matter, adding 72.4 ± 0.6% decrease for organic parameters. At the same time, the biological oxidation was also capable of providing high phenols removal, contributing to ~40% of the total phenols abatement. These two treatment stages attained a global removal efficiency of 93% for COD, 97% for TSS, and 97% for phenols, still requiring further treatment to comply with the respective ELVs.

For the third treatment stage, the PF-UVA process presented the highest organic matter removal (further 8 ± 1% – Fig. 6a and Table 2) and was the only AOP applied to the OMW that met the ELV for COD after 3 h of treatment (<150 mg O_2 L^{-1}, Table 2 and Fig. 6b). Regardless of the high process efficiency towards the organic parameters, along with additional removal of ~78% of aromatic compounds (UV_{254}, Table 2), it was still ineffective at fulfilling the remaining ELVs imposed (Fig. 6b and Table 2). Furthermore, the multistage treatment applying the PF-UVA process required pH acidification to 2.8, which resulted in a level of SO_4^{2-} exceeding the respective legal threshold since the pH correction was carried out with H_2SO_4. Another approach could be acidification with HCl. In addition, the PF-UVA process presents further

disadvantages related to the need of neutralizing the treated effluent, and the generation of sludge with high iron content.

In turn, AO was the least efficient AOP towards the organic matter, TSS, and color removal, although it obtained greater phenols removal than the PF-UVA process (Fig. 6a). The multistage treatment with AO presented a global removal > 92% for organic matter, phenols and TSS (Fig. 6a), but did not fulfill any of the respective ELVs.

Finally, the O_3 process contributed to the multistage treatment removing further 6.2 ± 0.8% of organic matter (Fig. 6a), which resulted in a treated effluent with COD values shortly above the ELV (167 mg O_2 L^{-1} – Fig. 6b). On that note, this AOP was also very efficient at decreasing the content of aromatic compounds (96% reduction for UV_{254}), which resulted in the distribution of organic matter mostly as non-humic compounds – $SUVA_{254}$ < 2 L mg^{-1} m^{-1} [71]. The combined strategy pre-treatment-coagulation-biological oxidation-O_3 for the treatment of undiluted OMW led to high removal of the remaining parameters (phenols = 99.7% and TSS ≈ 99%), for which the ELVs were met (phenols <0.5 mg L^{-1} and TSS <60 mg L^{-1}) (Fig. 6b and Table 2).

3.5.2. Operational cost estimation

Cost evaluation for the treatment train (Table 3) was calculated considering i) the experimental conditions applied for the different treatment stages, and ii) the costs in reagents and energy (further details in Tables SM-5 and −6). For the two initial treatment stages, coagulation and biological oxidation, a treatment cost of 1.20 € m^{-3} was estimated. The main costs associated with these well-known conventional treatment processes were: (i) the consumption of reagents (coagulation), (ii) sludge treatment and disposal (coagulation), and (iii) energy for aeration/agitation (biological oxidation). In literature, the operational cost for the coagulation of OMW, either using aluminum or ferric coagulants, has been reported in the range of 0.52–1.97 € m^{-3} [13,25,72], and the cost of a hybrid treatment aerobic biological treatment followed by coagulation/flocculation between 0.36 and 2.03 € m^{-3} [73].

For the most promising AOP options to be applied in the third stage of the treatment, i.e., PF-UVA (reaching legal compliance for COD) and O_3 (which reached the ELV for phenols, TSS, and does not compromise the sulfate limit), an operational cost of 5.2 € m^{-3} and 11.9 € m^{-3} was estimated, respectively (Table 3). For PF-UVA, the costs of (i) OMW neutralization, (ii) sludge treatment, and (iii) sludge disposal in a landfill were considered. This is in line with the economic analysis carried out by Cañizares, *et al.* [76], with the operational costs of O_3 being significantly higher than those of Fenton process. A cost of 3.15 $ m^{-3} (2.72 € m^{-3}) has been reported by Ahmed, *et al.* [15] for the PF-UVC treatment, considering only the oxidant and catalyst expenses (H_2O_2 = 3 g L^{-1} and Fe^{2+} = 30 mg L^{-1}), and are close to those obtained in this work (2.58 € m^{-3}). Likewise, Domingues, *et al.* [20] also pointed to reagents costs for the Fenton process of 2.8 € m^{-3} (1.44 € m^{-3} for H_2O_2 and 1.35 € m^{-3} for $FeSO_4$) for a OMW previously coagulated. Amaral-Silva, *et al.* [11], [77], for the combination of coagulation/-flocculation followed by Fenton, estimated an average treatment cost of 7.9 € m^{-3}, that was later reduced to 2.7 € m^{-3} at the industrial level.

According to the estimation, O_3 presented a treatment price 2.3-fold higher than PF-UVA. Operating cost savings (~33%) could be possible with system setup optimization (Gomes, *et al.* [34]), but values as low as for PF-UVA would not have been achieved. Implementing a subsequent and final biological treatment could be an option to lower the overall operating costs as a lower treatment time for the O_3 stage could be expected (further studies required). Also, even though the energy and chemicals costs in this study were accounted for industrial applications, the dosages optimized at the laboratory may be diminished for larger applications, as pointed by Amaral-Silva, *et al.* [77], further decreasing the treatment train costs (especially for the AOP stage) and making it more commercially attractive.

Table 3
Operational cost analysis for the different stages applied for the treatment of the OMW.

Treatment process	Reagent/ Energy cost (€ m^{-3})		
(1) Coagulation	$Al_2(SO_4)_3$	0.32	
	Sludge treatment and disposal[a]	0.39	
	Neutralization	0.25	
	(1) Total cost	0.96	
(2) Biological oxidation	Aeration energy[b]	0.14	
	Agitation energy	0.10	
	(2) Total cost	0.24	
		PF-UVA	**O_3**
(3) AOPs	H_2SO_4 (pH = 2.8)	0.15	–
	H_2O_2	2.4	–
	Energy	2.1	6.9
	$FeSO_4.7\ H_2O$	0.18	–
	Neutralization	0.30	–
	Sludge treatment and disposal[a]	0.08	–
	O_2	–	5.0
	(3) Total cost	5.2	11.9
Multistage	(1)+ (2)+ (3) Total cost	6.4	13.1

[a]Sludge treatment and disposal costs were based on Gomes, *et al.* [74];
[b]Considering 4.5 kg O_2 kWh^{-1} for aeration carried out by fine bubble diffusers [75].

4. Conclusions

A treatment train for the remediation of raw-undiluted OMW was investigated, intending to reach the limits for direct discharge into water bodies (namely for COD, phenols, and TSS) at a feasible cost. After a filtration/sedimentation pre-treatment for major oil/grease and solids/sludge removal, the OMW (pH = 4.5, turbidity = 4600 NTU, TSS = 4.0 g L^{-1}, COD = 10 g O_2 L^{-1}, and phenols = 164 mg L^{-1}) was remediated by a three-stage treatment comprising:

(i) For the first stage, a coagulation process using 0.8 g L^{-1} of $Al_2(SO_4)_3$ and keeping OMW natural pH (4.5), that mainly promoted removal of turbidity (98%), TSS (97%), and phenols (57%), decreasing the effluent toxicity (allowing a subsequent biological stage);
(ii) For the second stage, a biological oxidation, that mainly provided organic matter degradation (removal of 72% COD and 39% phenols);
(iii) For the third stage, after 3-h treatment the (a) PF-UVA treatment (pH = 2.8, $[H_2O_2]$ = 400–500 mg L^{-1}, $[TDI]_0$ = 100 mg L^{-1}) allowed to meet the discharge limits for COD but imposed constraints for legal compliance of other parameters, namely phenols, TSS, and sulfates; (b) O_3 process (OD_I = 20 mg O_3 min^{-1}) allowed meeting the discharge limits for phenols, TSS, and sulfates, and nearly complied with COD. The AO process proved to be the least efficient AOP towards the treatment of an OMW previously coagulated and biologically oxidated.

Although the strategy with O_3 in the AOP stage was the closest to meet the discharge limits for all studied parameters, it presents an operational cost 2.3-fold higher than PF-UVA (11.9 € m^{-3} *vs.* 5.2 € m^{-3}). Further research is required to assess the possibility of coupling a final biological treatment after the AOPs stage that could achieve full legal compliance and, simultaneously, decrease the overall treatment train costs.

CRediT authorship contribution statement

Srikanth Vuppala: Investigation, Validation. **Larissa O. Paulista:** Investigation, Validation, Writing – review & editing. **Daniela F.S. Morais:** Writing – original draft, Visualization, Investigation. **Inês L. Pinho:** Investigation. **Ramiro J.E. Martins:** Writing – review & editing.

Ana I. Gomes: Investigation, Conceptualization, Writing – original draft, Visualization, Writing – review & editing. **Francisca C. Moreira:** Conceptualization, Visualization, Writing – review & editing. **Vítor J.P. Vilar:** Conceptualization, Resources, Supervision, Writing – review & editing.

Declaration of Competing Interest

The authors declare that they have no known competing financial interests or personal relationships that could have appeared to influence the work reported in this paper.

Acknowledgments

This work was financially supported by (i) LA/P/0045/2020 (ALiCE), UIDB/50020/2020 and UIDP/50020/2020 (LSRE-LCM), funded by national funds through FCT/MCTES (PIDDAC), and (ii) Project NORTE-01-0247-FEDER-072124, *BagaÇo+Valor - Tecnologia Limpa para a Valorização dos Subprodutos do Bagaço na Indústria Extratora de Azeite*, funded by the European Regional Development Fund (ERDF). Srikanth Vuppala acknowledges the Joint Research Projects for the International Mobility of the XXXI and XXXII cycle PhD students for the project: CHEMBIOCAT, La Sapienza University of Rome. Larissa O. Paulista and Daniela F.S. Morais acknowledge their Ph.D. scholarships supported by FCT (SFRH/BD/137639/2018 and SFRH/BD/146476/2019, respectively). Francisca C. Moreira and Vítor J.P. Vilar acknowledge the FCT Individual Call to Scientific Employment Stimulus 2017 (CEECIND/02196/2017 and CEECIND/01317/2017, respectively).

Appendix A. Supporting information

Supplementary data associated with this article can be found in the online version at doi:10.1016/j.jece.2022.107442.

References

[1] International Olive Council (IOC), Economic affairs & promotion units - Figures. 2019.
[2] N. Rahmanian, S.M. Jafari, C.M. Galanakis, Recovery and removal of phenolic compounds from olive mill wastewater, J. Am. Oil Chem. Soc. 91 (2013) 1–18, https://doi.org/10.1007/s11746-013-2350-9.
[3] M. Dourou, A. Kancelista, P. Juszczyk, D. Sarris, S. Bellou, I.-E. Triantaphyllidou, A. Rywinska, S. Papanikolaou, G. Aggelis, Bioconversion of olive mill wastewater into high-added value products, J. Clean. Prod. 139 (2016) 957–969, https://doi.org/10.1016/j.jclepro.2016.08.133.
[4] International Olive Council (IOC), Newsletter nº 159. 2020.
[5] B.M. Esteves, C.S.D. Rodrigues, F.J. Maldonado-Hódar, L.M. Madeira, Treatment of high-strength olive mill wastewater by combined Fenton-like oxidation and coagulation/flocculation, J. Environ. Chem. Eng. 7 (2019), https://doi.org/10.1016/j.jece.2019.103252.
[6] S. Souilem, A. El-Abbassi, H. Kiai, A. Hafidi, S. Sayadi, C.M. Galanakis, Olive oil production sector: Environmental effects and sustainability challenges, Olive Mill. Waste (2017) 1–28, https://doi.org/10.1016/b978-0-12-805314-0.00001-7.
[7] A. Chiavola, G. Farabegoli, F. Antonetti, Biological treatment of olive mill wastewater in a sequencing batch reactor, Biochem. Eng. J. 85 (2014) 71–78, https://doi.org/10.1016/j.bej.2014.02.004.
[8] G. Hodaifa, P.A.R. Gallardo, C.A. García, M. Kowalska, M. Seyedsalehi, Chemical oxidation methods for treatment of real industrial olive oil mill wastewater, J. Taiwan Inst. Chem. Eng. 97 (2019) 247–254, https://doi.org/10.1016/j.jtice.2019.02.001.
[9] C.A. García, G. Hodaifa, Real olive oil mill wastewater treatment by photo-Fenton system using artificial ultraviolet light lamps, J. Clean. Prod. 162 (2017) 743–753, https://doi.org/10.1016/j.jclepro.2017.06.088.
[10] R. Elkacmi, M. Bennajah, Advanced oxidation technologies for the treatment and detoxification of olive mill wastewater: a general review, J. Water Reuse Desalination 9 (2019) 463–505, https://doi.org/10.2166/wrd.2019.033.
[11] N. Amaral-Silva, R.C. Martins, S. Castro-Silva, R.M. Quinta-Ferreira, Integration of traditional systems and advanced oxidation process technologies for the industrial treatment of olive mill wastewaters, Environ. Technol. 37 (2016) 2524–2535, https://doi.org/10.1080/09593330.2016.1153158.
[12] A.L. Ahmad, S. Sumathi, B.H. Hameed, Coagulation of residue oil and suspended solid in palm oil mill effluent by chitosan, alum and PAC, Chem. Eng. J. 118 (2006) 99–105, https://doi.org/10.1016/j.cej.2006.02.001.
[13] K. Kestioğlu, T. Yonar, N. Azbar, Feasibility of physico-chemical treatment and advanced oxidation processes (AOPs) as a means of pretreatment of olive mill effluent (OME), Process. Biochem. 40 (2005) 2409–2416, https://doi.org/10.1016/j.procbio.2004.09.015.
[14] M.S. Lucas, J.A. Peres, Removal of COD from olive mill wastewater by Fenton's reagent: Kinetic study, J. Hazard. Mater. 168 (2009) 1253–1259, https://doi.org/10.1016/j.jhazmat.2009.03.002.
[15] B. Ahmed, E. Limem, A. Abdel-Wahab, B. Nasr, Photo-Fenton treatment of actual agro-industrial wastewaters, Ind. Eng. Chem. Res. 50 (2011) 6673–6680, https://doi.org/10.1021/ie200266d.
[16] O. Chedeville, M. Debacq, C. Porte, Removal of phenolic compounds present in olive mill wastewaters by ozonation, Desalination 249 (2009) 865–869, https://doi.org/10.1016/j.desal.2009.04.014.
[17] P. Cañizares, J. Lobato, R. Paz, M.A. Rodrigo, C. Sáez, Advanced oxidation processes for the treatment of olive-oil mills wastewater, Chemosphere 67 (2007) 832–838, https://doi.org/10.1016/j.chemosphere.2006.10.064.
[18] M. Panizza, G. Cerisola, Olive mill wastewater treatment by anodic oxidation with parallel plate electrodes, Water Res 40 (2006) 1179–1184, https://doi.org/10.1016/j.watres.2006.01.020.
[19] M. Madani, M. Aliabadi, B. Nasernejad, R. Kermanj Abdulrahman, M. Yalili Kilic, K. Kestioglu, Treatment of olive mill wastewater using physico-chemical and Fenton processes, Desalin. Water Treat. 53 (2013) 2031–2040, https://doi.org/10.1080/19443994.2013.860882.
[20] E. Domingues, E. Fernandes, J. Gomes, S. Castro-Silva, R.C. Martins, Olive oil extraction industry wastewater treatment by coagulation and Fenton's process, J. Water Process Eng. 39 (2021), 101818, https://doi.org/10.1016/j.jwpe.2020.101818.
[21] L. Rizzo, G. Lofrano, M. Grassi, V. Belgiorno, Pre-treatment of olive mill wastewater by chitosan coagulation and advanced oxidation processes, Sep. Purif. Technol. 63 (2008) 648–653, https://doi.org/10.1016/j.seppur.2008.07.003.
[22] L. Ioannou-Ttofa, I. Michael-Kordatou, S.C. Fattas, A. Eusebio, B. Ribeiro, M. Rusan, A.R.B. Amer, S. Zuraiqi, M. Waismand, C. Linder, Z. Wiesman, J. Gilron, D. Fatta-Kassinos, Treatment efficiency and economic feasibility of biological oxidation, membrane filtration and separation processes, and advanced oxidation for the purification and valorization of olive mill wastewater, Water Res 114 (2017) 1–13, https://doi.org/10.1016/j.watres.2017.02.020.
[23] F.A. El-Gohary, M.I. Badawy, M.A. El-Khateeb, A.S. El-Kalliny, Integrated treatment of olive mill wastewater (OMW) by the combination of Fenton's reaction and anaerobic treatment, J. Hazard. Mater. 162 (2009) 1536–1541, https://doi.org/10.1016/j.jhazmat.2008.06.098.
[24] Y.B. Oz, H. Mamane, O. Menashe, V. Cohen-Yaniv, R. Kumar, L.I. Kruh, E. Kurzbaum, Treatment of olive mill wastewater using ozonation followed by an encapsulated acclimated biomass, J. Environ. Chem. Eng. 6 (2018) 5014–5023, https://doi.org/10.1016/j.jece.2018.07.003.
[25] S. Vuppala, I. Bavasso, M. Stoller, L. Di Palma, G. Vilardi, Olive mill wastewater integrated purification through pre-treatments using coagulants and biological methods: Experimental, modelling and scale-up, J. Clean. Prod. 236 (2019), https://doi.org/10.1016/j.jclepro.2019.117622.
[26] Decree Law 236/98, Ministry of the Environment. 1998, Official Gazette of Portugal. Series I-A no. 176, 1 August 1998.
[27] M. Achak, F. Elayadi, W. Boumya, Chemical coagulation/flocculation processes for removal of phenolic compounds from olive mill wastewater: a comprehensive review, Am. J. Appl. Sci. 16 (2019) 59–91, https://doi.org/10.3844/ajassp.2019.59.91.
[28] C.E. Santo, V.J.P. Vilar, C.M.S. Botelho, A. Bhatnagar, E. Kumar, R.A. R. Boaventura, Optimization of coagulation–flocculation and flotation parameters for the treatment of a petroleum refinery effluent from a Portuguese plant, Chem. Eng. J. 183 (2012) 117–123, https://doi.org/10.1016/j.cej.2011.12.041.
[29] F.C. Moreira, E. Bocos, A.G.F. Faria, J.B.L. Pereira, C.P. Fonte, R.J. Santos, J.C. B. Lopes, M.M. Dias, M.A. Sanromán, M. Pazos, R.A.R. Boaventura, V.J.P. Vilar, Selecting the best piping arrangement for scaling-up an annular channel reactor: an experimental and computational fluid dynamics study, Sci. Total Environ. 667 (2019) 821–832, https://doi.org/10.1016/j.scitotenv.2019.02.260.
[30] A.D. Webler, F.C. Moreira, M.W.C. Dezotti, C.F. Mahler, I.D.B. Segundo, R.A. R. Boaventura, V.J.P. Vilar, Development of an integrated treatment strategy for a leather tannery landfill leachate, Waste Manag. 89 (2019) 114–128, https://doi.org/10.1016/j.wasman.2019.03.066.
[31] W. Liu, S.A. Andrews, M.I. Stefan, J.R. Bolton, Optimal methods for quenching H_2O_2 residuals prior to UFC testing, Water Res 37 (2003) 3697–3703, https://doi.org/10.1016/S0043-1354(03)00264-1.
[32] F.C. Moreira, S. Garcia-Segura, R.A.R. Boaventura, E. Brillas, V.J.P. Vilar, Degradation of the antibiotic trimethoprim by electrochemical advanced oxidation processes using a carbon-PTFE air-diffusion cathode and a boron-doped diamond or platinum anode, Appl. Catal. B (2014) 492–505, https://doi.org/10.1016/j.apcatb.2014.05.052.
[33] C. Flox, P.L. Cabot, F. Centellas, J.A. Garrido, R.M. Rodríguez, C. Arias, E. Brillas, Solar photoelectro-Fenton degradation of cresols using a flow reactor with a boron-doped diamond anode, Appl. Catal. B 75 (2007) 17–28, https://doi.org/10.1016/j.apcatb.2007.03.010.
[34] A.I. Gomes, T.F. Soares, T.F.C.V. Silva, R.A.R. Boaventura, V.J.P. Vilar, Ozone-driven processes for mature urban landfill leachate treatment: organic matter degradation, biodegradability enhancement and treatment costs for different reactors configuration, Sci. Total Environ. 724 (2020), 138083, https://doi.org/10.1016/j.scitotenv.2020.138083.
[35] D. Mantzavinos, N. Kalogerakis, Treatment of olive mill effluents. Part I: organic matter degradation by chemical and biological processes — an overview, Environ. Int. 31 (2005) 289–295, https://doi.org/10.1016/j.envint.2004.10.005.

[36] K. Fadil, A. Chahlaoui, A. Ouahbi, A. Zaid, R. Borja, Aerobic biodegradation and detoxification of wastewaters from the olive oil industry, Int. Biodeterior. Biodegrad. 51 (2003) 37–41, https://doi.org/10.1016/s0964-8305(02)00073-2.
[37] Z.S. Lee, S.Y. Chin, J.W. Lim, T. Witoon, C.K. Cheng, Treatment technologies of palm oil mill effluent (POME) and olive mill wastewater (OMW): a brief review, Environ Technol. Innov. 15 (2019), https://doi.org/10.1016/j.eti.2019.100377.
[38] N. Gharsallah, Influence of dilution and phase-separation on the anaerobic-digestion of olive mill wastewaters, Bioprocess Eng. 10 (1994) 29–34, https://doi.org/10.1007/Bf00373532.
[39] J.M. Ochando-Pulido, S. Pimentel-Moral, V. Verardo, A. Martinez-Ferez, A focus on advanced physico-chemical processes for olive mill wastewater treatment, Sep. Purif. Technol. 179 (2017) 161–174, https://doi.org/10.1016/j.seppur.2017.02.004.
[40] X. Lu, Z. Chen, X. Yang, Spectroscopic study of aluminium speciation in removing humic substances by Al coagulation, Water Res 33 (1999) 3271–3280, https://doi.org/10.1016/s0043-1354(99)00047-0.
[41] J. Roussy, M. Van Vooren, E. Guibal, Chitosan for the coagulation and flocculation of mineral colloids, J. Dispers. Sci. Technol. 25 (2005) 663–677, https://doi.org/10.1081/dis-200027325.
[42] G. Enaime, A. Baçaoui, A. Yaacoubi, M. Wichern, M. Lübken, Olive mill wastewater pretreatment by combination of filtration on olive stone filters and coagulation–flocculation, Environ. Technol. 40 (2019) 2135–2146, https://doi.org/10.1080/09593330.2018.1439106.
[43] S. Vuppala, R.U. Shaik, M. Stoller, Multi-response optimization of coagulation and flocculation of olive mill wastewater: statistical approach, Appl. Sci. 11 (2021), https://doi.org/10.3390/app11052344.
[44] A. Fialová, E. Boschke, T. Bley, Rapid monitoring of the biodegradation of phenol-like compounds by the yeast Candida maltosa using BOD measurements, Int. Biodeterior. Biodegrad. 54 (2004) 69–76, https://doi.org/10.1016/j.ibiod.2004.02.004.
[45] H. El Hajjouji, L. El Fels, E. Pinelli, F. Barje, A. El Asli, G. Merlina, M. Hafidi, Evaluation of an aerobic treatment for olive mill wastewater detoxification, Environ. Technol. 35 (2014) 3052–3059, https://doi.org/10.1080/09593330.2014.930514.
[46] P. Paraskeva, E. Diamadopoulos, Technologies for olive mill wastewater (OMW) treatment: a review, J. Chem. Technol. Biot. 81 (2006) 1475–1485, https://doi.org/10.1002/jctb.1553.
[47] F. Haber, J. Weiss, The catalytic decomposition of hydrogen peroxide by iron salts, Proc. Math. Phys. Eng. Sci. 147 (1934) 332–351, https://doi.org/10.1098/rspa.1934.0221.
[48] Machulek, A., F.H., F. Gozzi, V.O., L. C, and J.E.F. Moraes, Fundamental mechanistic studies of the photo-Fenton reaction for the degradation of organic pollutants, in Organic Pollutants Ten Years After the Stockholm Convention - Environmental and Analytical Update. 2012.
[49] A.I. Gomes, S.G.S. Santos, T.F.C.V. Silva, R.A.R. Boaventura, V.J.P. Vilar, Treatment train for mature landfill leachates: optimization studies, Sci. Total Environ. 673 (2019) 470–479, https://doi.org/10.1016/j.scitotenv.2019.04.027.
[50] J.J. Pignatello, E. Oliveros, A. MacKay, Advanced oxidation processes for organic contaminant destruction based on the Fenton reaction and related chemistry, Crit. Rev. Environ. Sci. Technol. 36 (2006) 1–84, https://doi.org/10.1080/10643380500326564.
[51] L. Prieto-Rodríguez, I. Oller, A. Zapata, A. Agüera, S. Malato, Hydrogen peroxide automatic dosing based on dissolved oxygen concentration during solar photo-Fenton, Catal. Today 161 (2011) 247–254, https://doi.org/10.1016/j.cattod.2010.11.017.
[52] F. Torrades, J. García-Montaño, Using central composite experimental design to optimize the degradation of real dye wastewater by Fenton and photo-Fenton reactions, Dyes Pigments 100 (2014) 184–189, https://doi.org/10.1016/j.dyepig.2013.09.004.
[53] M. Panizza, G. Cerisola, Direct and mediated anodic oxidation of organic pollutants, Chem. Rev. 109 (2009) 6541–6569, https://doi.org/10.1021/cr9001319.
[54] D.C. Harris. Exploring Chemical Analysis, fourth ed., Basingstoke: W. H. Freeman, New York, 2009.
[55] P.A. Michaud, M. Panizza, L. Ouattara, T. Diaco, G. Foti, C. Comninellis, Electrochemical oxidation of water on synthetic boron-doped diamond thin film anodes, J. Appl. Electrochem 33 (2003) 151–154, https://doi.org/10.1023/A:1024084924058.
[56] L.W. Matzek, K.E. Carter, Activated persulfate for organic chemical degradation: a review, Chemosphere 151 (2016) 178–188, https://doi.org/10.1016/j.chemosphere.2016.02.055.
[57] P. Devi, U. Das, A.K. Dalai, In-situ chemical oxidation: principle and applications of peroxide and persulfate treatments in wastewater systems, Sci. Total Environ. 571 (2016) 643–657, https://doi.org/10.1016/j.scitotenv.2016.07.032.
[58] E. Chatzisymeon, N.P. Xekoukoulotakis, E. Diamadopoulos, A. Katsaounis, D. Mantzavinos, Boron-doped diamond anodic treatment of olive mill wastewaters: statistical analysis, kinetic modeling and biodegradability, Water Res 43 (2009) 3999–4009, https://doi.org/10.1016/j.watres.2009.04.007.
[59] J.H. Baxendale, J.A. Wilson, The photolysis of hydrogen peroxide at high light intensities, Trans. Faraday Soc. 53 (1957), https://doi.org/10.1039/tf9575300344.
[60] Beltrán, F.J., Ozone-UV Radiation-Hydrogen Peroxide Oxidation Technologies, in Chemical Degradation Methods for Wastes and Pollutants. 2003.
[61] L. Dogliotti, E. Hayon, Flash photolysis of per[oxydi]sulfate ions in aqueous solutions. The sulfate and ozonide radical anions, J. Phys. Chem. 71 (2002) 2511–2516, https://doi.org/10.1021/j100867a019.
[62] Y. Feng, D.W. Smith, J.R. Bolton, Photolysis of aqueous free chlorine species (HOCl and OCl^-) with 254 nm ultraviolet light, J. Environ. Eng. Sci. 6 (2007) 277–284, https://doi.org/10.1139/s06-052.
[63] F.C. Moreira, R.A.R. Boaventura, E. Brillas, V.J.P. Vilar, Electrochemical advanced oxidation processes: a review on their application to synthetic and real wastewaters, Appl. Catal. B 202 (2017) 217–261, https://doi.org/10.1016/j.apcatb.2016.08.037.
[64] F.J. Benitez, J. BeltranHeredia, J. Torregrosa, J.L. Acero, Improvement of the anaerobic biodegradation of olive mill wastewaters by prior ozonation pretreatment, Bioprocess Eng. 17 (1997) 169–175, https://doi.org/10.1007/s004490050371.
[65] D.R. Lide. CRC Handbook of Chemistry and Physics: A Ready-reference Book Of Chemical and Physical Data, eighty fourth ed., CRC Press, Boca Raton, 2003.
[66] D.A. Armstrong, R.E. Huie, W.H. Koppenol, S.V. Lymar, G. Merényi, P. Neta, B. Ruscic, D.M. Stanbury, S. Steenken, P. Wardman, Standard electrode potentials involving radicals in aqueous solution: Inorganic radicals (IUPAC Technical Report), Pure Appl. Chem. 87 (2015) 1139–1150, https://doi.org/10.1515/pac-2014-0502.
[67] I.D.B. Segundo, A.I. Gomes, B.M. Souza-Chaves, M. Park, A.B. dos Santos, R.A. R. Boaventura, F.C. Moreira, T.F.C.V. Silva, V.J.P. Vilar, Incorporation of ozone-driven processes in a treatment line for a leachate from a hazardous industrial waste landfill: Impact on the bio-refractory character and dissolved organic matter distribution, J. Environ. Chem. Eng. 9 (2021), https://doi.org/10.1016/j.jece.2021.105554.
[68] W.K. Lafi, B. Shannak, M. Al-Shannag, Z. Al-Anber, M. Al-Hasan, Treatment of olive mill wastewater by combined advanced oxidation and biodegradation, Sep. Purif. Technol. 70 (2009) 141–146, https://doi.org/10.1016/j.seppur.2009.09.008.
[69] R.C. Martins, A.M. Ferreira, L.M. Gando-Ferreira, R.M. Quinta-Ferreira, Ozonation and ultrafiltration for the treatment of olive mill wastewaters: effect of key operating conditions and integration schemes, Environ. Sci. Pollut. Res. 22 (2015) 15587–15597, https://doi.org/10.1007/s11356-015-4766-2.
[70] P. Karageorgos, A. Coz, M. Charalabaki, N. Kalogerakis, N.P. Xekoukoulotakis, D. Mantzavinos, Ozonation of weathered olive mill wastewaters, J. Chem. Technol. Biot. 81 (2006) 1570–1576, https://doi.org/10.1002/jctb.1490.
[71] D. Ghernaout, The hydrophilic/hydrophobic ratio vs. dissolved organics removal by coagulation – a review, J. King Saud. Univ. Sci. 26 (2014) 169–180, https://doi.org/10.1016/j.jksus.2013.09.005.
[72] B.K. Mert, T. Yonar, M.Y. Kiliç, K. Kestioğlu, Pre-treatment studies on olive oil mill effluent using physicochemical, Fenton and Fenton-like oxidation process, J. Hazard. Mater. 174 (2010) 122–128, https://doi.org/10.1016/j.jhazmat.2009.09.025.
[73] K. Pelendridou, M.M. Michailides, D.P. Zagklis, A.G. Tekerlekopoulou, C. A. Paraskeva, D.V. Vayenas, Treatment of olive mill wastewater using a coagulation-flocculation process either as a single step or as post-treatment efater aerobic biological treatment, J. Chem. Technol. Biot. 89 (2013), https://doi.org/10.1002/jctb.4269.
[74] A.I. Gomes, M.L.R. Foco, E. Vieira, J. Cassidy, T.F.C.V. Silva, A. Fonseca, I. Saraiva, R.A.R. Boaventura, V.J.P. Vilar, Multistage treatment technology for leachate from mature urban landfill: full scale operation performance and challenges, Chem. Eng. J. 376 (2019), https://doi.org/10.1016/j.cej.2018.12.033.
[75] Metcalf, I. Eddy, Wastewater engineering: Treatment and reuse. 4th ed. McGraw-Hill series in civil and environmental engineering. 2003, New York: McGraw-Hill. xxviii, 1819 p.
[76] P. Cañizares, R. Paz, C. Sáez, M.A. Rodrigo, Costs of the electrochemical oxidation of wastewaters: a comparison with ozonation and Fenton oxidation processes, J. Environ. Manag. 90 (2009) 410–420, https://doi.org/10.1016/j.jenvman.2007.10.010.
[77] N. Amaral-Silva, R.C. Martins, P. Nunes, S. Castro-Silva, R.M. Quinta-Ferreira, From a lab test to industrial application: scale-up of Fenton process for real olive mill wastewater treatment, J. Chem. Technol. Biot. 92 (2017) 1336–1344, https://doi.org/10.1002/jctb.5128.